Quaternary Science Reviews 30 (2011) 3109–3123

Contents lists available at ScienceDirect

Quaternary Science Reviews

journal homepage: www.elsevier.com/locate/quascirev

Structure and origin of Holocene cold events

Heinz Wanner [a,b,*], Olga Solomina [c], Martin Grosjean [a,b], Stefan P. Ritz [b,d], Markéta Jetel [a]

[a] Institute of Geography, University of Bern, Bern, Switzerland
[b] Oeschger Centre for Climate Change Research, University of Bern, Bern, Switzerland
[c] Institute of Geography, Russian Academy of Sciences, Moscow, Russia
[d] Climate and Environmental Physics, University of Bern, Bern, Switzerland

ARTICLE INFO

Article history:
Received 11 February 2011
Received in revised form
11 July 2011
Accepted 14 July 2011
Available online 10 August 2011

Keywords:
Holocene
Cold events
Bond cycles
Climate forcings
Climate atlas

ABSTRACT

The present interglacial, the Holocene, spans the period of the last 11,700 years. It has sustained the growth and development of modern society. The millennial-scale decreasing solar insolation in the Northern Hemisphere summer lead to Northern Hemisphere cooling, a southern shift of the Intertropical Convergence Zone (ITCZ) and a weakening of the Northern Hemisphere summer monsoon systems. On the multidecadal to multicentury-scale, periods of more stable and warmer climate were interrupted by several cold relapses, at least in the Northern Hemisphere extra-tropical area. Based on carefully selected 10,000-year-long time series of temperature and humidity/precipitation, as well as reconstructions of glacier advances, the spatiotemporal pattern of six cold relapses during the last 10,000 years was analysed and presented in form of a Holocene Climate Atlas (HOCLAT; see http://www.oeschger.unibe.ch/research/projects/holocene_atlas/). A clear cyclicity was not found, and the spatiotemporal variability of temperature and humidity/precipitation during the six specific cold events (8200, 6300, 4700, 2700, 1550 and 550 years BP) was very high. Different dynamical processes such as meltwater flux into the North Atlantic, low solar activity, explosive volcanic eruptions, and fluctuations of the thermohaline circulation likely played a major role. In addition, internal dynamics in the North Atlantic and Pacific area (including their complex interaction) were likely involved.

1. Introduction

The present interglacial, the Holocene, has sustained the growth and development of modern human society. It started about 11.7 ka BP with a rapid transition from the cold period called Younger Dryas to a subsequent, generally warmer period that showed relatively small amplitudes in the reconstructed temperature, but larger ones in tropical precipitation records (Dansgaard et al., 1989; Alley et al., 1993; Mayewski et al., 2004; Wanner et al., 2008). On the millennial timescale, the climate of the Holocene was strongly influenced by opposite hemispheric trends of the solar insolation during the corresponding summer, namely the decreasing insolation in the Northern and the increasing insolation in the Southern Hemisphere. This redistribution of energy lead to a southern shift of the Intertropical Convergence Zone (ITCZ) and a weakening of the Northern Hemisphere summer monsoon systems (Braconnot et al., 2007). On the multidecadal to multicentennial timescale, Holocene climate was variable and fluctuated between warm and cold, and humid and arid states. Based predominantly on studies of glacier fluctuations (Denton and Karlén, 1973; Thompson et al., 2009) and ice rafted debris (IRD) in the North Atlantic ocean (Bond et al., 1997, 2001) the question was raised whether these swings are cyclic or not, and whether or not a theory exists for their formation (Crowley, 2002; Alley, 2005; Debret et al., 2007).

The studies by Bond et al. (1997, 2001) stimulated the discussion and gave rise to a large number of publications. First the term "Bond cycle" was used to denote an oscillation during the last Ice Age whose period is equal to the time between successive Heinrich Events (Bond and Lotti, 1995; IPCC, 2001). In their following studies, Gerard Bond and co-authors endeavoured to find similar quasi–periodic cycles during the Holocene. They postulated the existence of a cycle with an average length of $\sim 1470 \pm 500$ years (Bond et al., 1997, 2001), and defined it as follows: "A prominent feature of the North Atlantic's Holocene climate is a series of shifts in ocean surface hydrography during which drift ice and cooler surface waters in the Nordic and Labrador Seas were repeatedly advected southward and eastward, each time penetrating deep into the warmer strands of the subpolar circulation". High peaks with fresh volcanic glass from Iceland or Jan Mayen and hematite stained

* Corresponding author. Oeschger Centre for Climate Change Research, University of Bern, Bern, Switzerland. Tel.: +41 31 631 3160; fax: +41 31 631 4338.
E-mail address: wanner@oeschger.unibe.ch (H. Wanner).

0277-3791/$ – see front matter © 2011 Elsevier Ltd. All rights reserved.
doi:10.1016/j.quascirev.2011.07.010

grains from eastern Greenland were interpreted to be the result of the southward and eastward advection of cold, ice-bearing surface waters from the Nordic and Labrador Seas during cold periods. In total nine Bond cycles were detected during the Holocene. Table 1 lists characterising keywords from the content of 30 papers published since 1995 that postulate a signal of one or more Bond events in their analysed time series. It demonstrates that the existence of Bond cycles is postulated for many areas of the Globe, in particular Europe, Asia and North America, yet one single theory explaining their formation has not been found (Debret et al., 2007; Wanner and Bütikofer, 2008). The most reported processes are changes in solar activity, changes in the dynamics of deep-water flow

Table 1
Overview on papers using natural archive data that refer to Bond-like cycles during the Holocene.

Reference	Location	Correlation with Bond cycles	Spectral peaks/cycle length	Possible mechanism
O'Brien et al. (1995)	Greenland (GISP 2)	0, 2, 4, 5, 8	Quasi 2600-year	Enhanced meridional atmospheric circulation
Bianchi and McCave (1999)	South Iceland basin	0–6	~1500-year periodicity	Changes in deep-water flow
Chapman and Shackleton (2000)	North Atlantic off Iceland	2, 5, 6, 7	Several spectral peaks	Cycles possibly driven by variation in solar activity
de Menocal et al. (2000a, b)	Off Cap Blanc, Mauretania	0–5, 7, 8	About every 1500 ± 500 yr	Increased southward advection of cooler waters or enhanced regional upwelling
Jennings et al. (2002)	East Greenland Shelf	1, 2, 3, 5	–	Increased flux of polar water and sea ice (changing NAO indices?)
Viau et al. (2002)	North America	Most cycles	1650 ± 500 yr	Abrupt transition between climatic regimes
Fleitmann et al. (2003)	Southern Oman	2–6	Several shorter cycles	Indian Ocean Monsoon precipitation responds to Bond events and to solar activity
Gupta et al. (2003)	Arabian Sea	1, 3, 4, 6, 7	–	Bond events coincide with weak Asian southwest monsoon (related to solar activity?)
Hong et al. (2003)	Tibetan Plateau	1, 3, 5, 7, 8	–	Thermohaline circulation decreases, SST decrease in North Atlantic and increase in Indian Ocean, monsoon weakens
Hu et al. (2003)	ArolikLake (SW Alaska)	3, 4, 6, 7, 8	Several spectral peaks (e.g. 590, 950 years)	Possible sun-ocean-climate link
Niggemann et al. (2003)	Sauerland (Germany)	Mainly cycles 1 and 2	1450 yr and minor peaks	Lower solar activity was probably accompanied by drier climate in northern Europe
Oppo et al. (2003)	Northeastern Atlantic Ocean	2, 4, 5, 6	Millennial oscillation of $\delta^{13}C$	Enhanced and reduced influence of NADW
Risebrobakken et al. (2003)	Eastern Norwegian Sea	0, 2, 4, 6, 7	No clear evidence for a cyclic behaviour	Stronger westerlies during early to mid-Holocene gave rise to eastward migration of subsurface Arctic water
Yu et al. (2003)	Continental western Canada	0–5	Broad band (mean: 1785 years)	Wet periods correlate with warm periods in the North Atlantic (response to solar activity?)
Hall et al. (2004)	Subpolar North Atlantic	0–3, 5, 6	Broad band of quasiperiodic variability	Link between the ISOW and the surface component of the MOC
Baker et al. (2005)	Lake Titicaca (South America)	1, 2, 4, 5	Several spectral peaks (e.g. 434–454 years)	Wet conditions on the Altiplano appear to be associated with cold conditions (Bond events) in the North Atlantic
Russell and Johnson (2005)	Lake Edward (Uganda/Congo)	0, 1	Enhanced power at ~725 years	Droughts in equatorial Africa occur during both, cold and warm events in the North Atlantic area
Gupta et al. (2005)	North-western Arabian Sea	0–7	Several significant peaks (e.g. at 1550, 152, 114 years)	Monsoon minima coincide with sunspot numbers and increased advection of drift ice in the North Atlantic area
Turney et al. (2005)	Northern Ireland	0, 2, 4, 5	Broad band of variability, cyclicity of ~800 yr	Trees collapse due to dryness during Bond events, but no response to changes in solar activity
Wang et al. (2005)	DonggeCave (southern China)	0–5	Peaks at 159 and 206 years	Correlation with ice rafted debris in the North Atlantic (influence of solar activity?)
Willard et al. (2005)	Chesapeake Bay (eastern North America)	1, 5	148, 177, 282, 1429 yr	Cold events in the North Atlantic are also effective in North America
Lamy et al. (2006)	Black Sea/Gulf of Aqaba	Partly	Cycles of ~500 and ~800 yr	AO/NAO-like atmospheric variability, likely originating from solar output changes
Moros et al. (2006)	Area off north Iceland	Partly	75–80 years, 1300 yr	Late Holocene trend in drift ice: Increasing in the cold East Current, decreasing in warmer North Atlantic Drift
Parker et al. (2006)	Southeastern Arabia	3, 4, 5	–	Decreasing precipitation during North Atlantic Bond events
Viau et al. (2006)	North America	0–2, 5	Periodicity of 1150 yr	Possibly solar forcing?
Yu et al. (2006)	Hexi Corridor (NW China)	0, 2, 5, 7, 8	–	Southward expansion of northern polar vortex, NAO index negative, ENSO pattern
Allen et al. (2007)	Finnmark, Norway	0, 1, 5	Several spectral peaks	Complex interaction between oceanic and atmospheric circulation, solar and tidal variability
Bendle and Rosell-Melé (2007)	North Icelandic Shelf	0, 2	–	No close correlation with Bond cycles, rather with NAO dynamics
Li et al. (2007)	WhiteLake (NE USA)	1–4	–	Dry intervals correlate with cold periods in the North Atlantic Ocean
Mangini et al. (2007)	Spannagel Cave	0, 2–5	–	Meteorological conditions in the European Alps respond synchronously to hydrographical changes in the North Atlantic

(including its interaction with sea ice) or teleconnections with the Indo-Pacific sea surface temperatures (SSTs), ENSO and the Asian monsoon systems (Emile-Geay et al., 2007). According to the review in Table 1, the cycles 2 (peak at ~3 ka BP) and 5 (showing a peak 5a at ~7.5 and a peak 5b at ~8.5 ka BP) are the most referred to in the 30 listed papers.

With the goal to get a more profound insight into the complex spatiotemporal structure of Holocene cold events we analyse a global set of Holocene time series from natural palaeoclimate archives which were selected based on specific quality criteria. We strictly leave out multimillennial-scale phenomena, focus on centennial-scale events and use an objective statistical procedure. In order to define the cold periods during the Holocene, suitable temperature proxies and glacier reconstructions are analysed. These data are supplemented by a specific set of humidity/precipitation proxy data, which enable determination of dry periods. As an additional result of our study, a Holocene Climate Atlas (HOCLAT; Wanner and Ritz, 2011) with graphics of the 46 analysed temperature and 35 humidity/precipitation proxy time series and 100 anomaly maps representing 100 year averages for the last 10,000 years was produced. This HOCLAT is available at: http://www.oeschger.unibe.ch/research/projects/holocene_atlas/.

2. Data and methods

The temperature and humidity/precipitation time series were selected and downloaded from official data repositories (e.g., NOAA World Data Center for Paleoclimatology), from scientific journals, put at our disposal by authors, or digitized from the published literature. Only records with a properly described methodology, a valuable age model, a precise site description, an average temporal resolution better than 160 years, and a temporal coverage of at least 70% of the defined Holocene period (10–0 ka BP) were used. If possible, annual means were included. The most challenging problem was to find a somewhat satisfactory spatial distribution of the data. In the case of questionable quality of a data set the decision was made following a thorough discussion among the co-authors of the paper and/or with the corresponding author(s) of the data set. Based on these quality criteria the majority of the ~500 data sets considered had to be eliminated.

The restriction to the last 10 ka was chosen due to the very small data availability prior to this period. Tables 2 and 3 show the lists of the temperature and humidity/precipitation proxies, including their characteristic features. Some time series only represent seasonal temperature or humidity/precipitation values. In this case

Table 2
List of the temperature proxies. Re: Temporal resolution.

	Type of temperature proxy	Record	Region	~Lat (deg)	~Long(deg)	~Re	Reference
1	Pollen (air temp., °C)	Lake sediment core	Sweden	60.83	15.83	108	Antonsson et al. (2006)
2	Chironomidae (July air temp., °C)	Lake sediment core	Sweden	68.37	18.7	79	Larocque and Hall (2004)
3	Pollen (July air temp., °C)	Lake sediment core	Finland	68.68	22.08	68	Seppä and Birks (2001)
4	Pollen (July air temp., °C)	Lake sediment core	Sweden	69.2	21.47	60	Seppä and Birks (2002)
5	Foram. MAT (August SST, °C)	Sea sediment core	Norway	66.97	7.63	72	Risebrobakken et al. (2003)
6	Pollen (Air temp., °C)	Lake sediment core	Finland	61.48	26.07	73	Heikkilä and Seppä (2003)
7	Pollen (Air temp., °C)	Lake sediment core	Sweden	58.55	13.67	98	Seppä et al. (2005)
8	Uk37 (SST, °C)	Sea sediment core	Gulf of Guinea	−5.6	−36.6	138	Schefuss et al. (2005)
9	Uk37 (SST, °C)	Sea sediment core	South China Sea	20.12	117.38	143	Pelejero et al. (1999)
10	Mg/Ca (SST, °C)	Sea sediment core	Southeast Atlantic	−25.5	13	104	Farmer et al. (2005)
11	Pollen (July air temp., °C)	Fossil pollen records	North America	57	−63	99	Viau et al. (2006)
12	Pollen (July air temp., °C)	Fossil pollen records	North America	55	−106	99	Viau et al. (2006)
13	Pollen (July air temp., °C)	Fossil pollen records	North America	43	−95	99	Viau et al. (2006)
14	Pollen (July air temp., °C)	Fossil pollen records	North America	64	−142	99	Viau et al. (2006)
15	Pollen (July air temp., °C)	Fossil pollen records	North America	35	−81	99	Viau et al. (2006)
16	Pollen (July air temp., °C)	Fossil pollen records	North America	37	−115	99	Viau et al. (2006)
17	Uk37 (Air temp., °C)	Sea sediment core	North West Africa	20.75	−18.58	80	Zhao et al. (1995)
18	d18O (Air temp., °C)	Ice core	GISP2, Greenland	72	−38	13	Alley (2000)
19	d18O from ostracods (‰)	Lake sediment core	Germany	47.1	11	35	von Grafenstein et al. (1999)
20	Uk37 (SST, °C)	Sea sediment core	Mediterranean	36.13	−2.62	120	Cacho et al. (2001)
21	Uk37 (SST, °C)	Sea sediment core	North Pacific	41.68	−124.93	129	Barron et al. (2003)
22	Mg/Ca (SST, °C)	Sea sediment core	Equatorial Pacific	6.3	125.83	49	Stott et al. (2007)
23	Mg/Ca (SST, °C)	Sea sediment core	Equatorial Pacific	−5	133.45	49	Stott et al. (2007)
24	Radiolarian (Summer SST, °C)	Sea sediment core	Nordic Sea	63.1	2.6	81	Dolven et al. (2002)
25	Mg/Ca (SST, °C)	Sea sediment core	Gulf of Guinea	2.5	9.38	40	Weldeab et al. (2007)
26	F13 (warm season SST, °C)	Sea sediment core	Subtropical Atlantic	20.75	−18.58	104	deMenocal et al. (2000a, b)
27	d18O (‰)	Speleothem	South Africa	−24.02	29.18	10	Holmgren et al. (2003)
28	dD (Temp. anomaly, °C)	Ice core	Vostok, Antarctica	−78	106	44	Petit et al. (1999)
29	dD (Temp., °C)	Ice core	EPICA Dome C, Antarctica	−75	123	18	Jouzel et al. (2007)
30	d18O (G. Bulloides, ‰)	Sea sediment core	Northeast Pacific	34.27	−120.07	14	Friddell et al. (2003)
31	d18O (N. Pachyderma, ‰)	Sea sediment core	Northeast Pacific	34.27	−120.07	14	Friddell et al. (2003)
32	d18O (‰)	Ice core	GRIP, Greenland	72	−37	4	Johnsen et al. (1997)
33	d18O (‰)	Speleothem	New Zealand	−41.33	172.22	40	Williams et al. (2005)
34	dD (‰)	Ice core	Taylor Dome, Antarctica	−77.8	158.72	30	Steig et al. (1998)
35	Soil bacteria (annual mean air temp., °C)	Lake sediment core	Congo River Basin	−5.58	11.22	136	Weijers et al. (2007)
36	d18O (‰)	Ice core	NGRIP, Greenland	76	−42	20	Vinther et al. (2006)
37	d18O (‰)	Ice core	Huascaran (Peru)	−9	−77.5	99	Thompson et al. (1995)
38	d18O (‰)	Ice core	Kilimanjaro	−3	37	50	Thompson et al. (2002)
39	d18O (‰)	Ice core	Agassiz ice cap	80	−73	25	Fisher and Koerner (1994)
40	Pollen (Coldest month temp., °C)	Lake sediment core	Lake Bajkal	52.78	108.12	130	Tarasov et al. (2009)
41	Pollen (Warmest month temp., °C)	Lake sediment core	Lake Bajkal	52.78	108.12	130	Tarasov et al. (2009)
42	(Summer SST, °C)	Sea sediment core	North Atlantic	60	−37	12	Mayewski et al. (2004)
43	TEX86 (SST, °C)	Sea sediment core	Antarctica	−64.86	−64.2	96	Shevenell et al. (2007)
44	d18O (Temp., °C)	Speleothem	Norway	66.62	13.68	34	Lauritzen and Lundberg (1999)
45	Pollen (Annual mean air temp., °C)	Lake sediment core	Estonia	58.58	26.65	98	Seppä and Poska (2004)
46	Uk37 (SST, °C)	Sea sediment core	North Pacific	36.03	141.78	66	Isono et al. (2009)

Table 3
List of the humidity/precipitation proxies (dig.: digitized time series).

	Type of humidity/precipitation proxy	Record	Region	~Lat(deg)	~Long(deg)	~Re	Reference
1	Accumulation rate (m ice/yr)	Ice core	GISP2, Greenland	72	−38	29	Alley (2000)
2	d18O (‰)	Lake sediment core	Canada	60.35	−134.8	22	Anderson et al. (2005)
3	Winter precipitation (% of present winter precipitation)	Lake sediment core	Norway	69.73	19.98	99	Bakke et al. (2005)
4	d18O (‰)	Speleothem	Oman	17.17	54.3	6	Fleitmann et al. (2007)
5	d18O (‰)	Speleothem	Oman	24.62	65.98	16	Staubwasser et al. (2003)
6	d18O (‰)	Speleothem	Dongee Cave, China	25.28	108.83	4	Wang et al. (2005)
7	d18O (‰)	Speleothem	Dongge Cave, China	25.28	108.83	15	Dykoski et al. (2005)
8	Ti (%)	Sea sediment core	Cariaco Basin	10.7	−65.17	6	Haug et al. (2001)
9	Precipitation (cm/yr)	Tree rings	Nevada, USA	37	−117	1	Hughes and Graumlich (1996)
10	Indian Ocean summer monsoon d13C (‰)	Peat bog sediment core	China	32.77	102.5	88	Hong et al. (2005)
11	East Asian summer monsoon d13C (‰)	Peat bog sediment core	Northeast China	42.22	126.52	24	Hong et al. (2005)
12	Plant macrofossil; detrended correspondence analysis (axis 1 scores)	Peat bog sediment core	Scotland	55.83	−3.43	75	Langdon et al. (2003)
13	Humification residuals (absorbance at 540 nm)	Peat bog sediment core	Scotland	55.83	−3.43	75	Langdon et al. (2003)
14	Water table depth (cm)	Peat bog sediment core	Scotland	55.83	−3.43	79	Langdon et al. (2003)
15	Precipitation (mm/yr)	Lake sediment core	Finland	69.2	21.47	60	Seppä and Birks (2002)
16	Relative lake level (Diatom principal component)	Lake sediment core	Lake Victoria	0.08	32.8	39	Stager et al. (2002)
17	Ti (1/s)	Lake sediment core	Lake Huguang Maar, China	22.5	110.28	1	Yancheva et al. (2007)
18	Annual mean precipitation (mm/yr)	Lake sediment core	Lake Bajkal	52.78	108.12	130	Tarasov et al. (2009)
19	Precipitation (mm/yr); dig.	Lake sediment core	Norway	61.75	7	110	Nesje et al. (2001)
20	Accumulation rate (cm ice/yr)	Ice core	Taylor Dome, Antarctica	−77	158	160	Steig et al. (2000)
21	Clay layer frequency (layers/200 yr)	Sea sediment core	Black Sea	41.54	31.17	50	Lamy et al. (2006)
22	Clay layer frequency (layers/200 yr)	Sea sediment core	Black Sea	41.17	31.09	52	Lamy et al. (2006)
23	CaCO3 (%)	Lake sediment core	Lake Chichancanab, Mexico	19.87	−88.77	22	Hodell et al. (1995)
24	Magnetic IRM ((A/m))	Sea sediment core	Eastern Mediterranean	34.07	32.72	73	Larrasoaña et al. (2003)
25	d18O (‰)	Speleothem	Indonesia	−8.53	120.43	10	Griffiths (2009)
26	d18O (‰)	Speleothem	Brazil	−27.22	−49.15	40	Wang et al. (2006)
27	Moisture index OUT OF d18O calcite and d18O ice (‰); dig.	Lake sediment core and ice core	Peru	−10	−76	143	Seltzer et al. (2000)
28	SSS (psu)	Sea sediment core	Gulf of Guinea	2.5	9.38	40	Weldeab et al. (2007)
29	d18O (‰)	Speleothem	China, Jiuxian Cave	33.57	109.1	10	Cai et al. (2010)
30	Precipitation (mm/yr); dig.	Speleothem	Heshang & Dongge Caves, China	28	110	110	Hu et al. (2008)
31	F-bSiO2 (g/m2 per year); dig.	Lake sediment core	Northeast China	42.28	126.6	63	Schettler et al. (2006)
32	Logarithm of pollen concentration (log(grains/g)); dig.	Lake sediment core	Northcentral, China	39	103.33	61	Chen et al. (2006)
33	Percentage of Picea and Pinus pollen (%); dig.	Lake sediment core	Northcentral, China	39	103.33	61	Chen et al. (2006)
34	d18O (‰)	Speleothem	China, Qixing Cave	26.07	107.25	70	Cai et al. (2001)
35	TOC (%); dig.	Lake sediment core	Mongolia	40.1	108.45	74	Chen et al. (2006)

the assessment of the annual mean value is restricted. The spatial distribution of the temperature and humidity/precipitation anomalies at the sites compiled in this study is represented in Fig. 4. The coordinates of the data sets representing a compilation of several records were arbitrarily chosen within the region of the study. Unfortunately, the lack of data in the Southern Hemisphere prohibited a meaningful regional subdivision of the data.

Since the focus is on centennial-scale changes, high-frequency variability was eliminated by applying a spline-fit according to Enting (1987) with a cut-off frequency of 1/500 yr^{-1}. Low-frequency variability was removed by detrending every data set using a spline-fit with 1/3000 yr^{-1} cut-off frequency. Fig. 1 shows examples of two analysed time series. We statistically define a cold or dry period as the time span where temperature or humidity/precipitation proxy values fall below one half of a standard deviation of the Holocene mean value (thus, approximately 30% of the data is within a cold or dry period; see the blue or brown segments in Fig. 1a and b). Analogously, warm or humid periods are defined (red or green segments in Fig. 1a and b). From the processed time series related to Fig. 1, the detected cold and dry events are first presented as a function of latitude (Fig. 2a and c). Also, the sum of the cold and dry events, respectively were calculated as a function of time (Fig. 3a and c). For this calculation the data was weighted inversely by the number of available data sets at the given time. The resulting curve was smoothed by a 50 yr moving average.

Glaciers are suitable qualitative indicators of regional and global cooling (Oerlemans, 2005). Therefore, a large set of available data detecting glacier advances was collected from the literature in Table 4 and represented in Fig. 2b. Where the glacier advance was provided as a range (black lines in Fig. 2b), the central date was used for the sum. Also, the beginning of a glacier advance (green circles with dashed line in Fig. 2b) or a best guess of it was used, respectively, when no other information was available or when the dating was imprecise (green circles with arrows in Fig. 2b). We have to consider that the dating of glacial deposits and landforms is very challenging (Winkler and Matthews, 2010). Most dates of the Holocene moraines are based on the radiocarbon analysis of organic material (buried or adjacent peat bogs, buried soils), which is not directly connected to the timing of the glacier advance. Therefore, we often obtain the minimum or maximum age of a moraine, which can differ from the date of the real advance by centuries or even millennia. Recently, novel methodologies, such as cosmogenic radionuclide dating (CRN, e.g., with ^{10}Be) of moraines, provide improved chronologies of glacier advances. In this study we

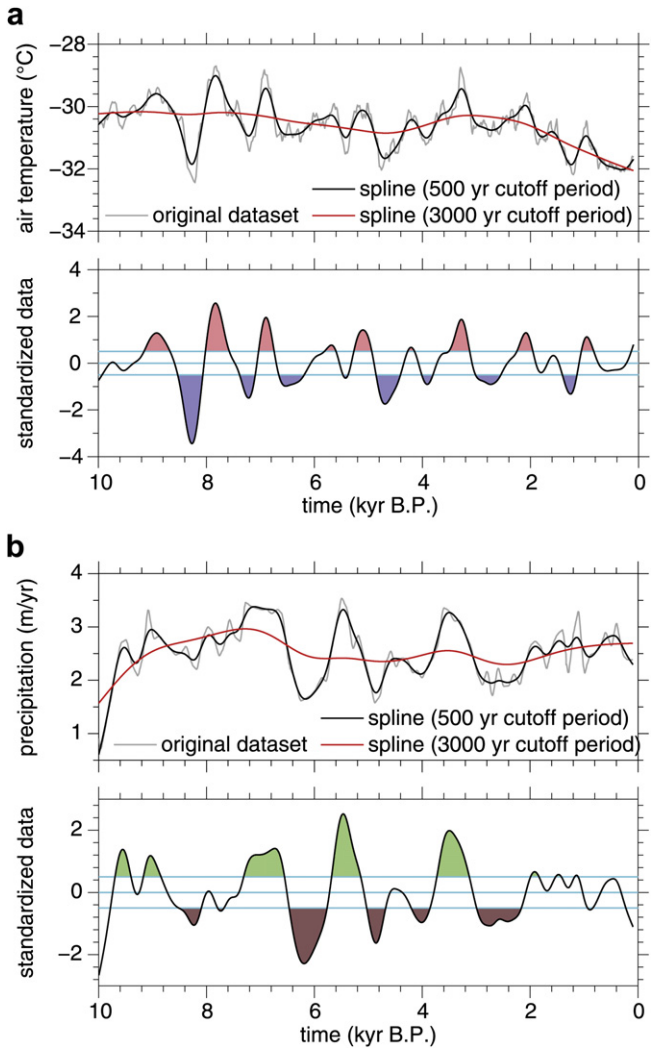

Fig. 1. Two time series representing a temperature reconstruction based on $\delta^{18}O$ data from the GISP 2 ice core (no. 18 in Table 2) and a reconstruction of annual precipitation based on a lake sediment core from Finland (no. 15 in Table 3). The upper curves show the original data, together with the splines for a 500-yr and a 3000-yr cut-off period. The lower curves show the smoothed time series after removing the millennial trend. The upper/lower blue curves represent an interval of ±0.5 standard deviation. A positive or negative (red or blue) anomaly of temperature or humidity/precipitation (green or brown) at a certain time was defined if the values lay above/below the upper/lower blue line. (For interpretation of the references to colour in this figure legend, the reader is referred to the web version of this article.)

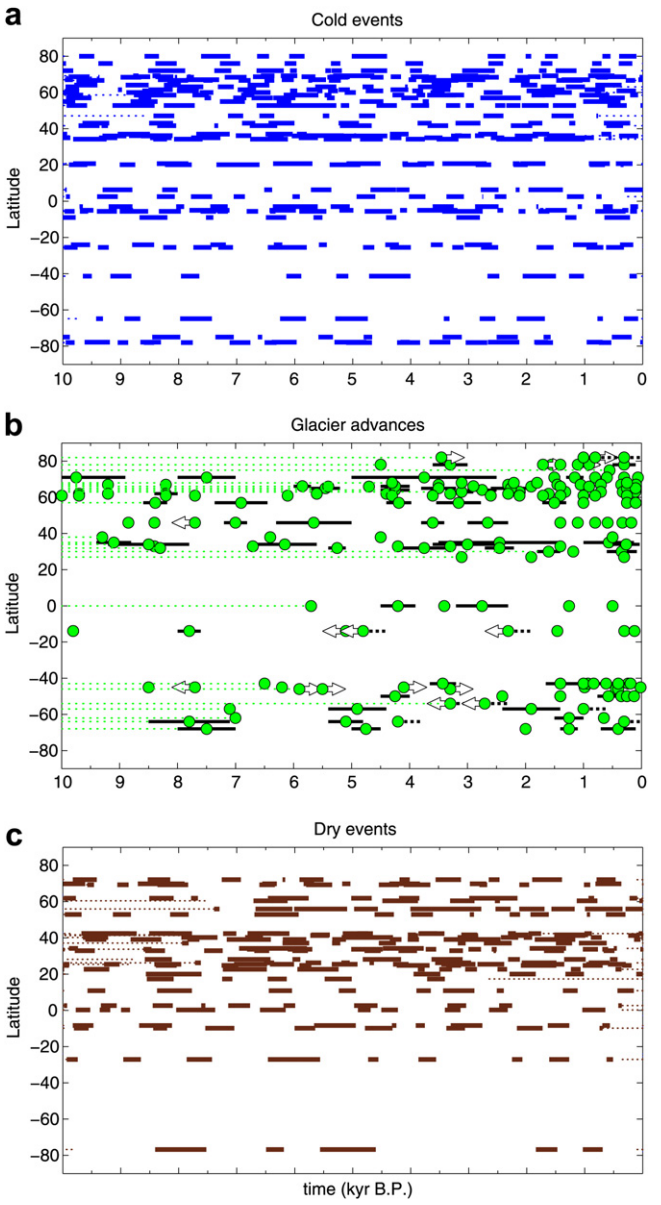

Fig. 2. (a) Blue horizontal bars representing cold periods based on the time series in Table 2. (b) Glacier advances based on the literature listed in Table 4. Advances of mountain glaciers are marked by green dots. Ranges of longer advance periods are indicated by black horizontal bars, and arrows mark possible advance periods. (c) Brown horizontal bars representing dry periods based on the time series in Table 3. (For interpretation of the references to colour in this figure legend, the reader is referred to the web version of this article.)

included two types of data on glacier variations: morphological discontinuous records based on the dated moraines, and continuous records from lake sediments of proglacial lakes. The continuous data provide the information on both advances and retreats, and statistical methods (e.g., detrending, correlation and wavelet analysis) are applied to treat these time series. Discontinuous data include dates of stadial moraines or sediments and landforms related to them. Discontinuous data provide less detailed information, however they can even be more reliable because they are based upon clear physical evidence. The history of glacier fluctuations is best understood using a combination of the two approaches (Osborn et al., 2007). It is impossible to estimate in a strict sense the precision of the dating of a glacier advance and retreat. It depends on the accuracy of the applied method, and on the local circumstances. The accuracy increases from the early to the late Holocene. An additional problem arises because it is difficult to distinguish between a readvance and a steady state behaviour of a glacier. In this paper we do not consider the scale of the registered glacier advances. In many cases it is unknown, uncertain, and not indicated in the original publications. We concentrated on information indicating a climate signal that triggered a glacier advance. Again, the sum of glacier advances was calculated by summing up all advances (green circles in Fig. 2b) within a 500-year window centred around the given time, and the data was weighted inversely by the number of available data sets at the given time (Fig. 3b).

3. Results

In the form of horizontal bars, the Fig. 2a and c show centennial-scale cold and dry anomalies as they were detected from the time series listed in Tables 2 and 3. The green dots and the black

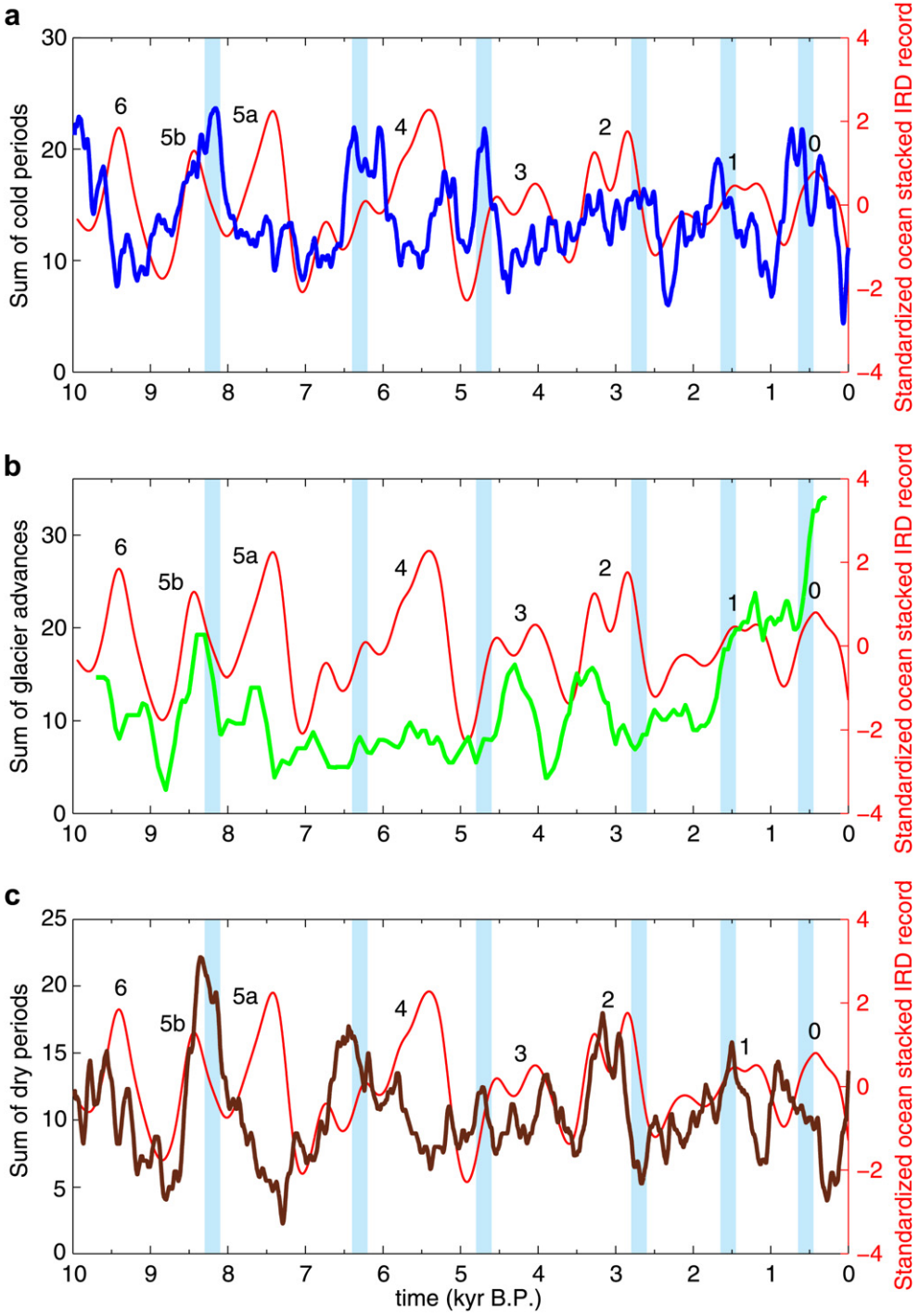

Fig. 3. (a) Weighted and smoothed curve (see method section) representing the sum of cold periods. (b) Same as (a) but for glacier advances. (c) Same as (a) but for dry periods. The red curves with the numbers in each Figure show the standardized ocean stacked ice rafted debris (IRD) record representing the Bond events no. 0–6 (Bond et al., 2001). The six vertical blue bars denote the time of the cold events represented by maps in Fig. 4. (For interpretation of the references to colour in this figure legend, the reader is referred to the web version of this article.)

horizontal bars in Fig. 2b represent the glacier advances determined from the data in the references listed in Table 4. The temporal resolution of the glacier reconstructions is low what hinders a precise global or inter-hemispheric interpretation of glacier advances and retreats (Winkler and Matthews, 2010). Already the study of the single curves in Fig. 1 and the Holocene Climate Atlas (HOCLAT) show that the spatiotemporal picture of the cold and dry events is very complex, yet concentrations of cold events are roughly discernible in Fig. 2a at about 8.2, 6.4 and 0.7 ka BP. An enhanced number of dry events occurred between 5.7 and 7.2 ka BP (Fig. 2c). An increasing number of Neoglacial glacier advances occurred after 4.5 ka BP.

A general overview of the temporal structure of cold and dry periods, as well as glacier advances, is represented by the curves in Fig. 3. As mentioned above, the sum of the cold and wet periods was weighted inversely by the number of available data sets at the given

Table 4
List of the proxies defining glacier advances.

Area	~Lat (deg)	References
Spitsbergen	78	Svendsen and Mangerud (1997), Werner (1993), Humlum et al. (2005)
Franz Josef Land	82	Lubinsky et al. (1999)
Novaya Zemlya	75	Polyak et al. (2004)
Greenland	59–83	Kelly and Lowell (2009), Ingòlfsson et al. (1990), Kelly (1988), Weidick et al. (2004), Weidick (1968), Weidick (1996), Geirsdottir et al. (2000), Bennike and Sparrenbom (2007)
Baffin Island	61–73	Miller (1973a), Miller (1973b), Miller et al. (2005), Briner et al. (2009)
Alaska (land-terminated glaciers)	54–71	Barclay et al. (2009)
S Iceland	66	Geirsdòttir et al. (2009)
Iceland (general)	63.5–66	Geirsdòttir et al. (2009)
Central Iceland	65	Kirkbride and Dugmore (2006)
Northern Iceland	64	Caseldine (1987), Caseldine and Stotter (1993), Stotter et al. (1999), Principato (2008)
Iceland, lakes	66	Hannesdóttir (2006), Geirsdóttir et al. (2007), Black (2008)
Scandinavia (general)	57–70	Nesje (2009)
Southern Norway	61	Matthews and Dresser (2008)
Northern Scandinavia	68	Rosqvist et al. (2004)
The Alps	44–47	Ivy-Ochs et al. (2009), Nicolussi and Patzelt (2001), Patzelt and Bortenschlager (1973), Bortenschlager (1970), Bortenschlager (1984), Patzelt (1977), Baroni and Orombelli (1996), Gamper and Suter (1982), Holzhauser (1995), Hormes et al. (1998), Hormes et al. (2001), Hormes et al. (2006), Holzhauser et al. (2005), Joerin et al. (2006), Joerin et al. (2008), King (1974), Schneebeli and Röthlisberger (2000), Zoller (1977), Röthlisberger et al. (1980), Bircher (1982), Bless (1982), Gamper and Oberhänsli (1982), Renner (1982), Zoller et al. (1966), Suter (1981), Furrer and Holzhauser (1989), Deline and Orombelli (2005), Holzhauser (1997), Röthlisberger and Oeschger (1961), Zumbühl and Holzhauser (1988), Zumbühl (1980), Holzhauser and Zumbühl (1999)
Western Canada	49–65	Menounos et al. (2009)
Tropical Andes	−8/−20	Glasser et al. (2009), Licciardi et al. (2006), Mark et al. (2002), Abbot et al. (2003), Rodbell (1992), Röthlisberger (1987), Solomina et al. (2007)
Central Chile and Argentina	−46	Espizua (2005)
N. Patagonian Ice Sheet	−46	Glasser et al. (2006), Douglass et al. (2005), Heusser (1960), Heusser (1964)
S. Patagonian Ice Sheet	−50	Mercer (1968), Ackert et al. (2008), Mercer (1982), Strelin and Malagnino (2000), Aniya (1995), Masiokas et al. (2008)
Cordillera Darwin	−54	Kuylenstierna et al. (1996)
New Zealand	−43	Schaefer et al. (2009)
Mt Kenia	0	Karlén et al. (1999)
Tibet	30–37	Yi et al. (2008)
Western Tibet	30–37	Seong et al. (2009)
Central and eastern Himalaya and SE Tibet	30	Yang et al. (2008)
Himalaya and Karakoram	27–37	Röthlisberger and Geyh (1985)
Northwestern China (continental glaciers)	35–40	Zhou et al. (1991)
Southeastern Tibet (maritime glaciers)	27	Zhou et al. (1991)
Western China including Tibet	27–40	Pu (1991), Lehmkuhl (1997)
Antarctic Peninsula and the adjacent South Atlantic islands (alpine glaciers)	−63/−73	Hall (2009)
South Shetland	−6/1−63	Hall (2009)
South Georgia	−56/−59	Rosqvist and Schuber (2003)
James Ross Island	−64	Strelin et al. (2006)

time and smoothed by a 50-yr moving average, and the sum of glacier advances was calculated by summing up all glacier advances (green circles in Fig. 2b) within a 500-yr window centred around the given time and weighted in a similar way. For comparison, the red curve of the ice rafted debris (IRD) record by Bond et al. (2001) is added in all three Figures. Multicentury-scale variability is obvious in all represented time series. If we consider all three phenomena, cold periods, glacier advances and Bond cycles together, roughly six remarkable cold events can be distinguished during the last 10 ka BP. They are represented by blue bars in Fig. 3, in form of individual maps in Fig. 4, and characterized in Table 5. The cold events from 8.6 to 8.0 and 3.3–2.5 ka BP, as well as for the Little Ice Age from 1250 to 1850 AD, correlate best with the Bond events 5b, 2 and 1 (Fig. 3a). Interestingly, a high number of time series with dry anomalies occurred during the two earliest cold events as well as during the so-called Dark Age Cooling (Ljungqvist, 2010) from 300 to 600 AD (nr. 1, 2 and 5 in Table 5). Conversely, an average to low number of dry anomalies was registered during the other three periods, including the Little Ice Age (Grove, 2004) from 1250 to 1850 AD (no. 3, 4 and 6 in Table 5). The patterns of the cold events 3 and 4 (Table 5) show the highest diversity. With 800 years, event 4 spans the longest time period.

As mentioned above, the maps with all 100-year averages of temperature and humidity/precipitation anomalies for the last 10 ka are represented in the Holocene Climate Atlas (HOCLAT). Fig. 4 shows six selected global maps with the 200-yr averages represented for the climax of the six cold events listed in Table 5. In contrast to the Figures in the HOCLAT a 200-yr average was chosen to get a more stable picture of the corresponding cold event. For both temperature and humidity/precipitation, the data are divided into the three categories high, average and low. As expected the patterns show a very complex picture. Even though a certain number of positive temperature anomalies (red dots) becomes apparent, all six patterns show predominantly negative ones. Only event 4 around 3.3–2.5 ka BP (Fig. 4d) indicates that several positive temperature anomalies occurred, mainly in the Northern Hemisphere. A remarkable opposite tendency in all patterns appears in the area of Scandinavia and its surroundings, which

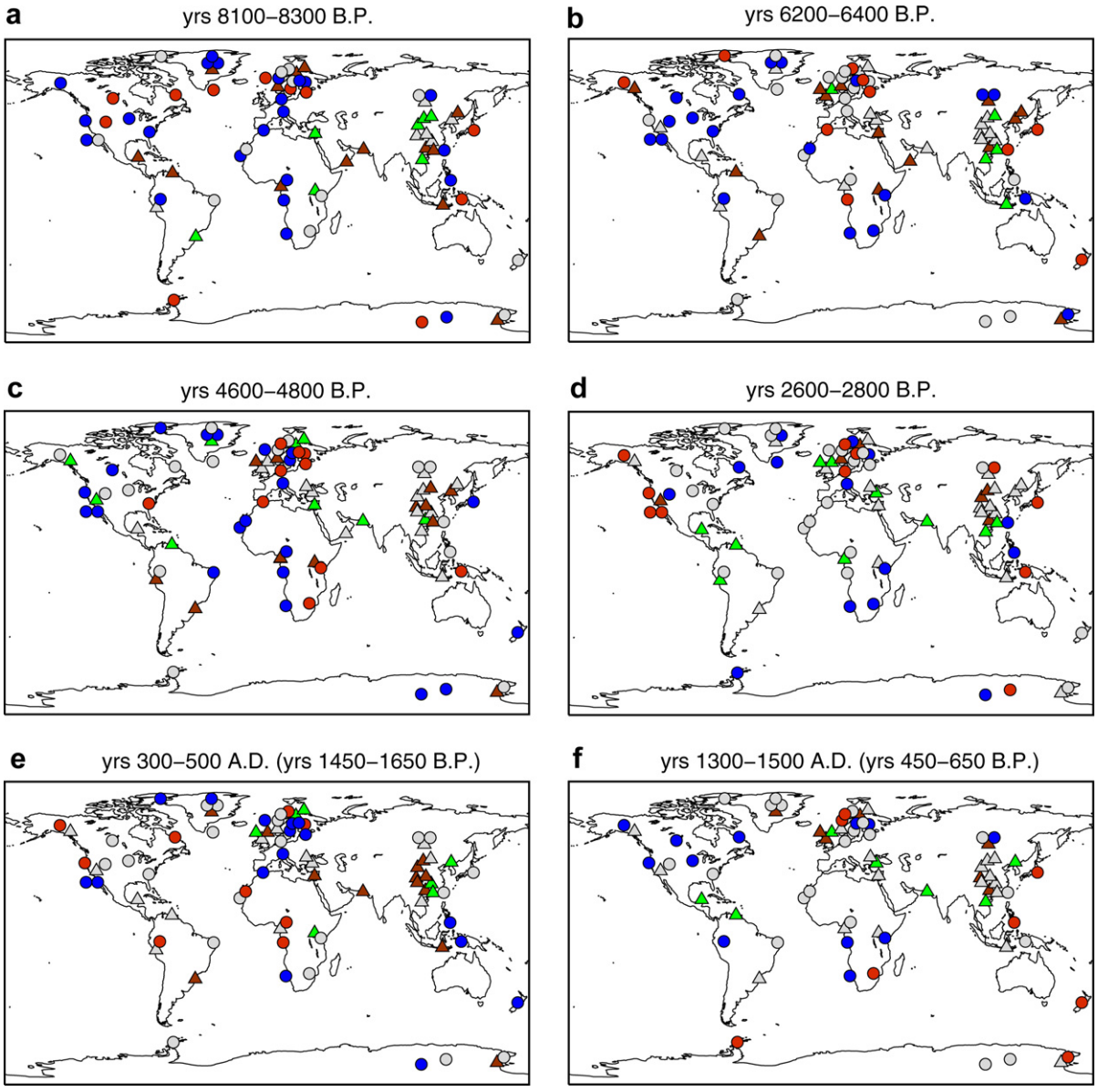

Fig. 4. Maps representing the six distinct cold relapses during the Holocene (see the blue bars in Figs. 3 and 5). Red dots show positive and blue dots negative temperature anomalies. Green triangles represent positive and brown triangles negative humidity/precipitation anomalies. Grey colours depict average values. For reasons of clarity, coordinates of overlapping records in map figures may have been shifted slightly. (For interpretation of the references to colour in this figure legend, the reader is referred to the web version of this article.)

show a high number of positive temperature anomalies during all cold events except event 5, the Dark Age or Migration Period Cooling which lasted from 300 to 600 AD. The tendency for positive temperature anomalies is mainly visible in the time series 1, 4 and 45 in Table 2 and is also confirmed by regional studies (Seppä et al., 2007). As already mentioned, dryness prevailed during the cold events 1, 2 and 5 (Table 5), mainly in the Northern Hemisphere. Due to the sparse information we have in the Antarctic area a clear statement for this region is not possible.

Table 5
Characteristics of the six cold events represented in Fig. 4.

Time slice according to Figs. 3 and 4 (ka BP)	Length of cold period (ka BP; see Fig. 3a)	Sum of cold periods	Sum of glacier advances	Sum of dry periods
1) 8.3–8.1	8.6–8.0	High	High	High
2) 6.4–6.2	6.5–5.9	High	Average	High
3) 4.8–4.6	4.8–4.5	High	Low	Average
4) 2.8–2.6	3.3–2.5	Average	Average	Average
5) 1.65–1.45 (300–500 AD)	1.75–1.35 (300–600 AD)	High	Average	High
6) 0.65–0.45 (1300–1500 AD)	0.7–0.15 (1250–1850)	High	High	Average

4. Discussion

It has to be asked how much the patterns in Figs. 2–4 were determined by important climate forcing factors or by the effects of internal variability. For this reason the time series of the four most important climate forcing factors are represented in Fig. 5. In addition, the six distinct cold periods indicated in Fig. 4 and Table 5 are marked by blue bars. Even though the focus of this contribution lies on the multicentury timescale, it has to be stressed that at the millennial timescale, the Holocene climate was dominated by the influence of summer season orbital forcing, represented in Fig. 5a.

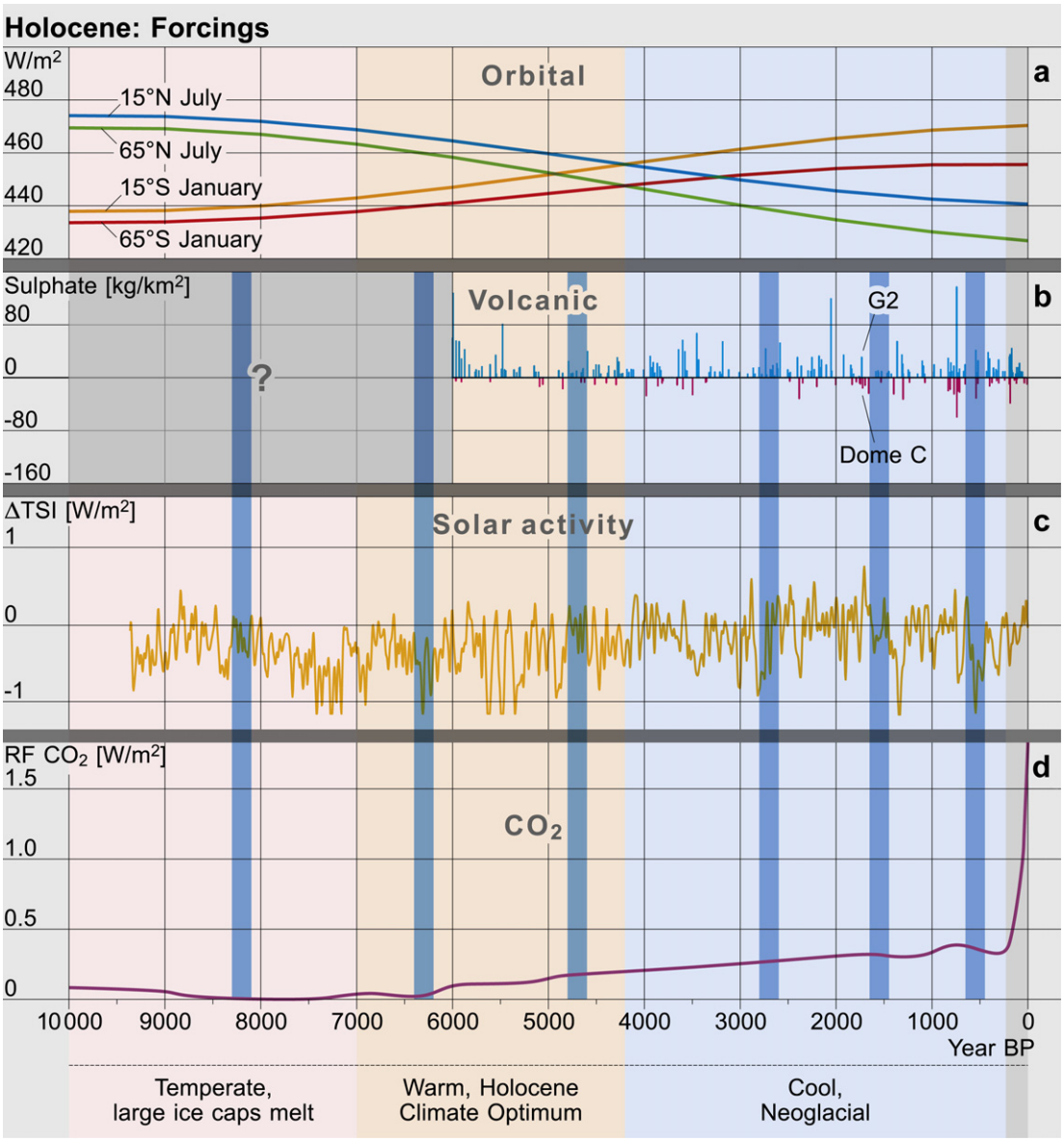

Fig. 5. Main forcings during the Holocene. (a) Solar insolation due to orbital changes for two specific sites in the Northern and Southern Hemispheres during the corresponding summer (Berger, 1978). (b) Volcanic forcing during the past 6 ka depicted by the sulphate concentrations of two ice cores from Greenland (blue vertical bars) and Antarctica (red vertical bars; Wanner et al., 2008). (c) Solar activity fluctuations reconstructed based on ^{10}Be measurements in polar ice (Steinhilber et al., 2009). (d) Forcing due to rising CO_2 concentrations (IPCC, 2007). The six vertical blue bars indicate the timing, but not the length of the six cold periods indicated in the six maps in Fig. 4. (For interpretation of the references to colour in this figure legend, the reader is referred to the web version of this article.)

The summer insolation curves of both hemispheres for the last 10 ka show opposite behaviour, where the Northern Hemisphere insolation decreased by almost 40 W m^{-2} (and vice versa). Therefore, a strong shift in the hemispheric temperature distribution, as well as in the intensity of the monsoon systems, was observed (Mayewski et al., 2004; Wanner et al., 2008). Based on these facts the Holocene can be divided into three main periods. The first period between approximately 11.7 and 7 ka BP is characterised by a high summer insolation in the Northern Hemisphere, still a cool or temperate climate mainly in the surroundings of the melting ice sheets in North America and Eurasia (Renssen et al., 2009), and a high monsoon activity in Africa (de Menocal et al., 2000b) and Asia (Zhang et al., 2011). The second period between about 7 and 4.2 ka BP marks the so-called Holocene Thermal Maximum (also called 'Holocene Climate Optimum', 'Altithermal' or 'Hypsithermal' from a Northern Hemisphere viewpoint). Compared to the preindustrial period prior to year 1900 AD this period was clearly characterised by higher summer temperatures in the Northern Hemisphere mid- and high-latitude areas (Klimenko et al., 1996; Alverson et al., 2003), and most of the global monsoon systems were still active, but weakening (Wang et al., 2005; Huang et al., 2008; Wanner et al., 2008; Zhang et al., 2011). The third period, called 'Neoglaciation' or 'Neoglacial', was dominated by decreasing summer temperatures in the Northern Hemisphere due to decreasing insolation during the boreal summer (Porter and Denton, 1967; Denton and Karlén, 1973). Even though summer insolation in the Northern Hemisphere decreased after the mid-Holocene, there is evidence from some areas that not only the Holocene Thermal Maximum (Masson et al., 2000; Kaufman et al., 2006) but also the Neoglacial period started earlier (Kelly and Lowell, 2009). The Neoglacial was terminated by

global warming, which at the beginning of the 20th century was most likely induced by the increasing anthropogenic greenhouse effect (IPCC, 2007; Fig. 5d).

Because our study is centred on multidecadal- to multicentury-scale temperature fluctuations, clusters of volcanic eruptions and solar irradiance, above all during periods they coincide, play an important role. Unfortunately a sound volcanic data set representing spatiotemporal changes in aerosol optical depth covering the whole Holocene period is not available (Gao et al., 2008). The blue and red vertical lines in Fig. 5b suggest that the highest number of strong tropical volcanic eruptions likely occurred during the last cold event no. 6, the Little Ice Age (Wanner et al., 2008). A few long-term reconstructions of solar activity exist (Krivova and Solanki, 2008; Steinhilber et al., 2009). Although the reconstructions indicate that the amplitude of solar activity fluctuations was rather small and some age models can still be questioned, the curve in Fig. 5c shows that phases of low (high) solar activity often coincided with periods of lower (higher) temperatures (Gray et al., 2010). This does not necessarily mean that solar activity was the main trigger behind the formation of all Holocene cold events because other processes, such as explosive tropical volcanic eruptions, fluctuations of the ocean thermohaline circulation or internal feedbacks, might also have played an important role (Wanner et al., 2008). Internal variability is particularly relevant with regard to regional or local climate signals (Bengtsson et al., 2006), and therefore, for many of the existing reconstructions from proxy archives.

In order to get further insight into the dynamics of the formation of Holocene cold events, the above mentioned six significant cold relapses (see the vertical bars in Figs. 3 and 5 as well as Table 5) were analysed. The global maps showing temperature (circles) and humidity/precipitation (triangles) anomalies for these selected periods are displayed in Fig. 4. Positive (negative) temperature anomalies are shown in red (blue), positive (negative) humidity anomalies in green (brown). Grey dots or triangles represent average conditions (see the method Section 2 and Tables 2 and 3). It is important to note that all time series were detrended and show relative anomalies in the variability band from centuries up to one millennium at maximum. They do not, therefore, represent multimillennial-scale phenomena. Note that the curves of cold events are significantly correlated with those of the warm events ($r = -0.55$). The same is valid for the dry and humid events ($r = -0.45$). The correlations between cold (warm) and dry (humid) events amount to $r = 0.44$ (0.52).

Fig. 4a shows the pattern for the well known 8.2 ka BP cold event, which coincides roughly with Bond event 5b (see Fig. 3 or Bond et al., 1997, 2001). This event followed a longer time period from 9.5 to about 8.6 ka BP with mostly positive temperature. It has been the focus of a large number of studies (e.g., Alley et al., 1997; Alley and Ágústsdóttir, 2005; Rohling and Pälike, 2005; Cheng et al., 2009). The majority of temperature proxies indicate negative temperature anomalies. Dryness predominated in Latin America and parts of the Indian and Asian monsoon areas. Several warm anomalies are indicated for North America, parts of Scandinavia, Japan and the tropical west Pacific, and two of the three stations in Antarctica (Fig. 4a). This rather complex spatiotemporal pattern could also be due to the fact that different regions reacted with a different timelag to the cooling influence of the still existent, but strongly melting Laurentide ice sheet (Renssen et al., 2009). Rohling and Pälike (2005) show that different cooling events occurred in different regions over a period of 400–600 years. Based on alkenone-derived sea surface temperatures Kim et al. (2004) have demonstrated that a negative (positive) sea surface temperature trend is indicated during the mid- to late Holocene for the north-eastern Atlantic (northeastern Pacific). While the solar activity curve shows only a very weak minimum around 8.4 ka BP (Fig. 5c), the 8.2 ka BP cooling event was most likely triggered by a downturn of the thermohaline circulation in the North Atlantic due to the meltwater outflow from the continental ice sheets, mainly from the Laurentide area (Barber et al., 1999; Alley and Ágústsdóttir, 2005; Rohling and Pälike, 2005; Renssen et al., 2007; Carlson et al., 2008). Based on stalagmite records, Cheng et al. (2009) show that an antiphase pattern existed with a weak summer monsoon in Asia and an intensified summer monsoon in South America, a pattern that also appears in simulations with meltwater pulses in the North Atlantic (LeGrande and Schmidt, 2008).

The second cooling event, represented in Fig. 4b, occurred between 6.5 and 5.9 ka BP (i.e., after the beginning of the Holocene Thermal Maximum). Similar to the 8.2 ka BP event, a predominance of negative temperature anomalies existed in the Southern Hemisphere, a majority of positive temperature anomalies occurs around Scandinavia but, contrary to Fig. 4a, the inner area of North America was cool. Kaufman et al. (2004) show that the warming during the Holocene Thermal Maximum was time-transgressive across the western Arctic, and northeastern Canada remained cool for another few millennia due to the residual Laurentide Ice Sheet. According to Fig. 5c solar activity was clearly reduced. The maps in the HOCLAT show that a remarkable dryness existed in the Asian monsoon area between about 6900 and 6300 years BP. It is argued that the East Asian monsoon was extremely weak during this cold event, due to a cold North Atlantic area and a southward shift of the ITCZ (Xiao et al., 2009). Zhang et al. (2011) demonstrate that the monsoon activity was not weak, but clearly declining during this period. Another interesting hypothesis is that ENSO acts as a mediator of low solar influence and drives ocean circulation in the North Atlantic to produce Bond-like events (Emile-Geay et al., 2007). In contrast, some authors even report a moderate to warm climate in Europe and even for the whole Northern Hemisphere mid- and high-latitudes (Alverson et al., 2003).

The event which occurred between 4.8 and 4.5 ka BP (Fig. 4c) coincides roughly with Bond event 3 (Fig. 3) and is indicated by negative temperature anomalies in Greenland, North America, Africa and Antarctica. Again, most time series in northern Europe showed average conditions or even positive temperature anomalies. Positive humidity anomalies occurred in the Northern Hemisphere, except eastern Asia. The maps in the HOCLAT show strong changes during the whole 4th millennium BP with even more negative temperature anomalies between 4.8 and 4.6 ka BP. Around 4.7 ka BP solar activity was average (Fig. 5c). The peak in the frequency curve of the glacier advances was reached later (around 4.3 ka BP), itself marking the transition to the Neoglacial period (Fig. 3b). Interestingly, several authors relate this cooling period to strong dryness in North America (Booth et al., 2005) and the collapse of the old Akkadian culture in Mesopotamia (Weiss et al., 1993), as well as the collapse of old Chinese cultures (An et al., 2005).

The fourth cool event depicted in Fig. 4d occurred between 3.3 and 2.5 ka BP (Table 5) and corresponds with Bond event 2 (Fig. 3). Not least because of its long duration the pattern was variable and complex. Similar to the 4.7 ka BP event, Fig. 4d shows that almost no warm anomaly occurred in the Southern Hemisphere (van Geel et al., 2000). This cooling event also coincided with a remarkable low solar activity forcing (Fig. 5c). In addition, some authors postulate that this solar signal was amplified by the thermohaline circulation and was therefore also prominently detected in proxy time series from Eurasia (Speranza et al., 2002; Plunkett et al., 2004; van Geel et al., 2004; Swindles et al., 2007). Fig. 4d also indicates positive temperature anomalies in Scandinavia and northwestern America, and dryness in the northern Asian monsoon area. Based on the HOCLAT maps the European time series showed a number of negative temperature anomalies prior to this event. After 2.4 ka BP a large number of positive anomalies occurred at the global scale.

The fifth cold event, which occurred between 1.75 and 1.35 ka BP (300–600 AD; Fig. 4e), is also known as Dark Age or Migration Period Cooling (Ljungqvist, 2010). This period marked the transition from Late Antiquity to the Early Middle Ages, and a strong human migration occurred roughly between the years 300–700 AD in Europe. The curve with the frequency of cold events (Fig. 3a) shows a clear peak around 400 AD, and the highest number of negative temperature anomalies of all six cold events was observed during this period in the European area. Rather warm conditions existed in Africa. The frequencies of the glacier advances (Fig. 3b) increased remarkably, and dryness prevailed in the Arabian and parts of the Asian area. Interestingly, the solar forcing curve on Fig. 5c shows a negative peak shortly after this event, and a larger volcanic activity also started after 600 AD (Zielinski, 2000). Further studies have to examine whether or not this was due to inaccurate age models.

Based on our statistical analysis the last cold period, the Little Ice Age (LIA; Fig. 4f), occurred between 0.7 and 0.15 ka BP (1200–1800 AD). In many studies the LIA encompasses the time period between the 14th and the 19th century (Matthews and Briffa, 2005). It represents the archetype of a Holocene cold relapse (Grove, 2004), corresponds well with Bond event 0 and correlates with a series of Grand Solar Minima (Fig. 5c) as well as a high number of strong tropical volcanic eruptions (Fig. 5b). Some authors (Mann et al., 2009; Trouet et al., 2009) argue that the transition from the warmer Medieval Climate Anomaly (Hughes and Diaz, 1994; Bradley et al., 2003) to the LIA was due to a shift to a mostly negative mode of the North Atlantic Oscillation. The pattern in Fig. 4f, again representing a 200-year average, covers a large part of one of the coldest subperiods during the LIA, encompassing the Wolf and the Spörer Minimum. The map shows a predominant number of negative or average temperature anomalies. At least in many areas of the Northern Hemisphere outer tropics, the Little Ice Age was likely the coldest multidecadal to multicentury long Holocene period since the 8.2 ka BP event (Wanner et al., 2008; Kaufman et al., 2009). Several authors argue that a lower solar activity additionally triggered the slowdown of the thermohaline circulation in the North Atlantic (Renssen et al., 2007). Reconstructions of solar activity minima and large volcanic eruptions (Fig. 5) show a remarkable sychronization of those events, and simulations based on related data show that the Little Ice Age was characterised by an alternation of warmer and cooler periods (IPCC, 2007). This behaviour is also visible in glacier reconstructions from different continents (Clague et al., 2009). Mainly in Europe, the LIA is associated with societal reactions, e.g. the disappearance of the Norse colonies in Greenland or the abandonment of permanent settlements in the Alps (Pfister, 1995; Fagan, 2000; Grove, 2004).

5. Conclusions

The Holocene can roughly be divided into three periods (early deglaciation phase, Holocene Thermal Optimum, Neoglacial period). Based on a statistical analysis of proxy time series we demonstrate that, at the multidecadal to multicentury timescale, several cold relapses interrupted periods of relatively stable and warmer climate. Our results show that their appearance was not strictly regular or cyclic, and one single process cannot explain their complex spatiotemporal pattern. Most likely decreasing solar insolation, combined with a possible slowdown of the thermohaline circulation and, in some cases, also combined with a series of tropical volcanic eruptions, may have played an essential role. In addition, feedback effects may have been important. This is particularly important if regional or even local phenomena are considered (Bengtsson et al., 2006), which is the case for many proxy time series. Based on the fact that the summer insolation decreased strongly during the Northern Hemisphere (boreal) summer (Wanner et al., 2008) and that temperature was low in the late Holocene at least in the Arctic area (Kaufman et al., 2009) the question must be raised whether we would still remain in the Little Ice Age or at least early 19th century climate regime today, if anthropogenic climate change had not masked the natural driving forces of the climate system. The rapidly growing number of studies will help to answer this question.

Acknowledgements

We thank the two anonymous reviewers who helped to improve this paper. We also thank Alex Hermann for graphical support, Sarina Scheidegger and Daniel Gähwiler for data collection, Eva Baumgartner and Laura Hobi for preparation of the references, and Krystyna Saunders and Louise Newman for the proofreading of the text.

References

Abbott, M.B., Wolfe, B.B., Wolfe, A.P., Seltzer, G.O., Aravena, R., Mark, B.G., Polissar, P.J., Rodbell, D.T., Rowe, H.D., Vuille, M., 2003. Holocene paleohydrology and glacial history of the central Andes using multiproxy lake sediment studies. Palaeogeogr. Palaeoecol. 194, 123–138.

Ackert Jr., R.P., Becker, R.A., Singer, B.S., Kurz, M.D., Caffee, M.W., Mickelson, D.M., 2008. Patagonian glacier response during the Late Glacial-Holocene transition. Science 321, 392–395.

Allen, J.R.M., Long, A.J., Ottley, C.J., Pearson, D.G., Huntley, B., 2007. Holocene climate variability in northernmost Europe. Quaternary Sci. Rev. 26, 1432–1453.

Alley, R.B., Ágústsdóttir, A.M., 2005. The 8k event: cause and consequences of a major Holocene abrupt climate change. Quaternary Sci. Rev. 24, 1123–1149.

Alley, R.B., 2000. The Younger Dryas cold interval as viewed from central Greenland. Quaternary Sci. Rev. 19, 213–226.

Alley, R.B., 2005. Abrupt climate changes, oceans, ice and us. Oceanography 17, 194–204.

Alley, R.B., Mayewski, P.A., Sowers, T., Stuiver, M., Taylor, K.C., Clark, P.U., 1997. Holocene climate instability: a prominent widespread event 8200 yr ago. Geology 25, 483–486.

Alley, R.B., Meese, D.A., Shuman, C.A., Gow, A.J., Taylor, K.C., Grootes, P.M., White, J.W.C., Ram, M.E., Waddington, E.D., Mayewski, P.A., Zielinski, G.A., 1993. Abrupt increase in Greenland snow accumulation at the end of the Younger Dryas event. Nature 362, 527–529.

Alverson, K.D., Bradley, R.S., Pedersen, T.F., 2003. Paleoclimate, Global Change and the Future. Springer, New York.

An, C.-B., Tang, L., Barton, L., Chen, F.-H., 2005. Climate change and cultural response around 4000 cal yr B.P. in the western part of Chinese Loess Plateau. Quaternary Res. 63, 347–352.

Anderson, A., Abbott, M.B., Finney, B.P., Burns, S.J., 2005. Regional atmospheric circulation change in the North Pacific during the Holocene inferred from lacustrine carbonate oxygen isotopes, Yukon Territory, Canada. Quaternary Res. 64, 21–35.

Aniya, M., 1995. Holocene glacial chronology in Patagonia: Tyndall and Upsala glaciers. Arctic Alpine Res. 27, 311–322.

Antonsson, K., Brooks, S.J., Seppä, H., Telford, R.J., Birks, H.J.B., 2006. Quantitative palaeotemperature records inferred from fossil pollen and chironomid assemblages from Lake Gilltjärnen, northern central Sweden. J. Quaternary Sci. 21, 831–884.

Baker, P.A., Fritz, S.C., Garland, J., Ekdahl, E., 2005. Holocene hydrologic variation at Lake Titicaca, Bolicia/Peru, and its relationship to North Atlantic climate variation. J. Quaternary Sci. 20, 655–662.

Bakke, J., Dahl, S.O., Paasche, Ø, Løvlie, R., Nesje, A., 2005. Glacier fluctuations, equilibrium-line altitudes and palaeoclimate in Lyngen, northern Norway, during the Lateglacial and Holocene. Holocene 15, 518–540.

Barber, D.C., Dyke, A., Hillaire-Marcel, C., Jennings, A.E., Andrews, J.T., Kerwin, M.W., Bilodeau, G., McNeely, R., Southon, J., Morehead, M.D., Gagnon, J.-M., 1999. Forcing of the cold event of 8,200 years ago by catastrophic drainage of Laurentide lakes. Nature 400, 344–348.

Barclay, D.J., Wiles, G.C., Calkin, P.E., 2009. Holocene glacier fluctuations in Alaska. Quaternary Sci. Rev. 28, 2034–2048.

Baroni, C., Orombelli, G., 1996. The alpine "Iceman" and holocene climatic change. Quaternary Res. 46, 78–83.

Barron, J.A., Heusser, L., Herbert, T., Lyle, M., 2003. High-resolution climatic evolution of coastal northern California during the past 16,000 years. Paleoceanography 18, 1020.

Bendle, J.A.P., Rosell-Melé, A., 2007. High-resolution alkenone sea surface temperature variability on the North Icelandic Shelf: implications for Nordic Seas palaeoclimate development during the Holocene. Holocene 17, 9–24.

Bengtsson, L., Hodges, K.I., Roeckner, E., Brokopf, R., 2006. On the natural variability of the pre-industrial European climate. Clim. Dynam 27, 743–760.

Bennike, O., Sparrenbom, C.J., 2007. Dating of the Narssarssuaq stade in southern Greenland. Holocene 17, 279–282.
Berger, A., 1978. Long-term variations of daily insolation and Quaternary climate changes. J. Atmos. Sci. 35, 2362–2367.
Bianchi, G.G., McCave, I.N., 1999. Holocene periodicity in North Atlantic climate and deep ocean flow south of Iceland. Nature 397, 515–517.
Bircher, W., 1982. Zur Gletscher- und Klimageschichte des Saastales. Phys. Geographie 9, 1–233.
Black, J., 2008. Holocene climate change in south central Iceland: a multiproxy lacustrine record from glacial lake Hvitarvatn. Ph. D. thesis, University of Colorado, Boulder.
Bless, R., 1982. Beiträge zur spät- und postglazialen Geschichte der Gletscher im nordöstlichen Mont Blanc Gebiet. Phys. Geographie 15, 1–116.
Bond, G.C., Lotti, R., 1995. Iceberg discharges into the North Atlantic on millennial time scales during the last glaciation. Nature 267, 1005–1010.
Bond, G., Kromer, B., Beer, J., Muscheler, R., Evans, M.N., Showers, W., Hoffmann, S., Lotti-Bond, R., Hajdas, I., Bonani, G., 2001. Persistent solar influence on North Atlantic climate during the Holocene. Science 278, 1257–1266.
Bond, G., Showers, W., Cheseby, M., Lotti, R., Almasi, P., de Menocal, P., Priore, P., Cullen, H., Hajdas, I., Bonani, G., 1997. A pervasive millennial-scale cycle in the North Atlantic Holocene and glacial climates. Science 294, 2130–2136.
Booth, R.K., Jackson, S.T., Forman, S.L., Kutzbach, J.E., Bettis III, E.A., Kreig, J., Wright, D.K., 2005. A severe centennial-scale drought in mid-continental North America 4200 years ago and apparent global linkages. Holocene 15, 321–328.
Bortenschlager, S., 1984. Beiträge zur Vegetationsgeschichte Tirols I. Inneres Ötztal und unteres Inntal. Ber. des naturw.-med. Vereins Innsbruck 71, 19–56.
Bortenschlager, S., 1970. Waldgrenz- und Klimaschwankungen im pollenanalytischen Bild des Gurgler Rotmooses. Mitteilg. d. Ostalpin-Dinarischen Gesellschaft f. Vegetationskd 11, 19–26.
Braconnot, P., Otto-Bliesner, B., Harrison, S., Joussaume, S., Peterchmitt, J.-Y., Abe-Ouchi, A., Crucifix, M., Driesschaert, E., Fichefet, T., Hewitt, C.D., Kageyama, M., Kitoh, A., Laîné, A., Loutre, M.-F., Marti, O., Merkel, U., Ramstein, G., Valdes, P., Weber, S.L., Yu, Y., Zhao, Y., 2007. Results of PMIP2 coupled simulations of the Mid-Holocene and Last Glacial Maximum – Part 1: experiments and large-scale features. Clim. Past 3, 261–277.
Bradley, R.S., Hughes, M.K., Diaz, H.F., 2003. Climate in Medieval time. Science 302, 404–405.
Briner, J.P., Davis, P.T., Miller, G.H., 2009. Latest Pleistocene and holocene glaciation of Baffin Island, Arctic Canada: key patterns and chronologies. Quaternary Sci. Rev. 28, 2075–2087.
Cacho, I., Grimalt, J.O., Canals, M., Sbaffi, L., Shackelton, N.J., Schönfeld, J., Zahn, R., 2001. Variability of the western Mediterranean Sea surface temperature during the last 25,000 years and its connection with the Northern Hemisphere climatic changes. Paleoceanography 16, 40–52.
Cai, Y., Tan, L., Cheng, H., An, Z., Edwards, R.L., Kelly, M.J., Kong, X., Wang, X., 2010. The variation of summer monsoon precipitation in central China since the last deglaciation. Earth Planet. Sc. Lett. 291, 21–31.
Cai, Y., Zhang, M., Peng, Z., Lin, Y., An, Z., Zhang, Z., Cao, Y., 2001. The δ18O variation of a stalagmite from Qixing Cace Province and indicated climate change during the Holocene. Chin. Sci. Bull. 46, 1904–1908.
Carlson, A.E., Legrande, A.N., Oppo, D.W., Came, R.E., Schmidt, G.A., Anslow, F.S., Licciardi, J.M., Obbink, E.A., 2008. Rapid early Holocene deglaciation of the Laurentide ice sheet. Nat. Geosci. 1, 620–624.
Caseldine, C.J., 1987. Neoglacial glacier variation in Northen Iceland. Examples from the Eyjafjordur. Arctic Alpine Res. 19, 296–305.
Caseldine, C., Stotter, J., 1993. Little Ice Age glaciation of Trollaskagi peninsula, northern Iceland: climatic implications for reconstructed equilibrium line altitudes (ELAs). Holocene 3, 357–366.
Chapman, M.R., Shackleton, N.J., 2000. Evidence of 550-year and 1000-year cyclicities in North Atlantic circulation patterns during the Holocene. Holocene 10, 287–291.
Chen, F.-H., Cheng, B., Zhao, Y., Zhu, Y., Madsen, D.B., 2006. Holocene environmental change inferred from a high-resolution pollen record, Lake Zhuyeze, arid China. Holocene 16, 675–684.
Cheng, H., Fleitmann, D., Edwards, L.R., Wang, X., Cruz, F.W., Auler, A.S., Mangini, A., Wang, Y., Kong, X., Burns, S.J., Matter, A., 2009. Timing and structure of the 8.2 ky event inferred from δ18O records of stalagmites from China, Oman and Brazil. Geology 37, 1007–1010.
Clague, J.J., Menounos, B., Osborn, G., Luckman, B.H., Koch, J., 2009. Nomenclature and resolution in Holocene glacial chronologies. Quaternary Sci. Rev. 28, 2231–2238.
Crowley, T.J., 2002. Cycles, cycles, everywhere. Science 295, 1473–1474.
Dansgaard, W., White, J.W.C., Johnsen, S.J., 1989. The abrupt termination of the Younger Dryas climate event. Nature 339, 532–534.
Debret, M., Bout-Roumazeilles, V., Grousset, F., Desmet, M., McManus, J.F., Massei, N., Sebag, D., Petit, J.-R., Copard, Y., Trentesaux, A., 2007. The origin of the 1500-year climate cycles in Holocene North-Atlantic records. Clim. Past 3, 569–575.
Deline, P., Orombelli, G., 2005. Glacier fluctuations in the western Alps during the Neoglacial, as indicated by the Miage morainic amphitheatre (Mont Blanc massif, Italy). Boreas 34, 456–467.
deMenocal, P., Ortiz, J., Guilderson, T., Sarnthein, M., 2000a. Coherent high and low latitude climate variability during the Holocene warm period. Science 288, 2198–2202.
deMenocal, P., Ortiz, J., Guilderson, T., Adkins, J., Sarnthein, M., Baker, L., Yarusinsky, M., 2000b. Abrupt onset and termination of the Africal Humid Period: rapid climate responses to gradual insolation forcing. Quaternary Sci. Rev. 19, 347–361.
Denton, G.H., Karlén, W., 1973. Holocene climatic variations - Their pattern and possible cause. Quaternary Res. 3, 155–205.
Dolven, J.K., Cortese, G., Bjorklund, K.R., 2002. A high-resolution radiolarian-derived paleotemperature record for the Late Pleistocene-Holocene in the Norwegian Sea. Paleoceanography 17, 1072.
Douglass, D.C., Singer, B.S., Kaplan, M.R., Ackert, R.P., Mickelson, D.M., Caffee, M.W., 2005. Evidence of early Holocene glacial advances in southern South America from cosmogenic surface-exposure dating. Geology 33, 237–240. 2005.
Dykoski, C.A., Edwards, R.L., Cheng, H., Yuan, D., Cai, Y., Zhang, M., Lin, Y., Qing, J., An, Z., Revenaugh, J., 2005. A high-resolution, absolute-dated Holocene and deglacial Asian monsoon recordfrom Dongge Cave, China. Earth Planet. Sci. Lett. 233, 71–85.
Emile-Geay, J., Cane, M., Seager, R., Kaplan, A., Almasi, P., 2007. El Niño as a mediator of the solar influence on climate. Paleoceanography 22. doi:10.1029/2006PA001304.
Enting, I.G., 1987. On the use of smoothing splines to filter CO2 Data. J. Geophys. Res. 92, 10,977–10,984.
Espizua, L., 2005. Holocene glacier chronology of Valenzuela valley, Mendoza Andes, Argentina. Holocene 15, 1079–1085.
Fagan, B.M., 2000. The Little Age: how climate made history, 1300–1850. Amazon.
Farmer, E.C., deMenocal, P.B., deMenocal, P.B., Marchitto, T.M., 2005. Holocene and deglacial ocean temperature variability in the Benguela upwelling region: implications for low latitude atmospheric circulation. Paleoceanography 20, PA2018.
Fisher, D.A., Koerner, R.M., 1994. Signal and noise in four ice-core records from Agassiz Ice Cap, Ellesmere Island, Canada: details of the last millennium for stable isotopes, melt and solid conductivity. Holocene 4, 113–120.
Fleitmann, D., Burns, S.J., Mangini, A., Mudelsee, M., Kramers, J., Villa, I., Neff, U., Al-Subbary, A.A., Buettner, A., Hippler, D., Matter, A., 2007. Holocene ITCZ and Indian monsoon dynamics recorded in stalagmites from Oman and Yemen (Socotra). Quaternary Sci. Rev. 26, 170–188.
Fleitmann, D., Burns, S.J., Mudelsee, M., Neff, U., Kramers, J., Mangini, A., Matter, A., 2003. Holocene forcing of the Indian monsoon recorded in a stalgmite from Southern Oman. Science 300, 1737–1739.
Friddell, J.E., Thunell, R.C., Guilderson, T.P., Kashgarian, M., 2003. Increased northeast Pacific climatic variability during the warm middle Holocene. Geophys. Res. Lett. 30, 1560–1574.
Furrer, G., Holzhauser, H., 1989. 2500 Jahre Gletschergeschichte der Schweizer Alpen. Akademie der Wissenschaften und der Literatur Mainz, Stuttgart, pp. 144–160.
Gamper, M., Oberhänsli, H., 1982. Interpretation von Radiocarbondaten fossiler Böden. Phys. Geographie 1, 83–90.
Gamper, M., Suter, J., 1982. Postglaziale Klimageschichte der Schweizer Alpen. Geogr. Helv. 37, 105–114.
Gao, C., Robock, A., Ammann, C., 2008. Volcanic forcing of climate over the past 1500 years: an improved ice core-based index for climate models. J. Geophys. Res. 113. doi:10.1029/2008JD010239.
Geirsdóttir, A., Hardardóttir, J., Andrews, J.T., 2000. Late-Holocene terrestrial glacial history of Miki and I.C. Jacobsen Fjords, East Greenland. Holocene 10, 123–134.
Geirsdóttir, A., Miller, G.H., Andrews, J.T., 2007. Glaciation, erosion, and landscape evolution of Iceland. J. Geodyn 43, 170–186.
Geirsdóttir, A., Miller, G.H., Axford, Y., Olafsdòttir, S., 2009. Holocene and latest Pleistocene climate and glacier fluctuations in Iceland. Quaternary Sci. Rev. 28, 2107–2118.
Glasser, N.F., Clemmens, S., Schnabel, C., Fenton, C.R., McHargue, L., 2009. Tropical glacier fluctuations in the Cordillera Blanca, Peru between 12.5 and 7.6 ka from cosmogenic 10Be dating. Quaternary Sci. Rev. 28, 3448–3458.
Glasser, N.F., Harrison, S., Ivy-Ochs, S., Duller, G.A.T., Kubik, P.W., 2006. Evidence from the Rio Bayo valley on the extent of the north Patagonian Icefield during the late Pleistocene-holocene transition. Quaternary Res. 65, 70–77.
Gray, L.J., Beer, J., Geller, M., Haigh, J.D., Lockwood, M., Matthes, K., Cubasch, U., Fleitmann, D., Harrison, G., Hood, L., Luterbacher, J., Meehl, G.A., Shindell, D., van Geel, B., White, W., 2010. Solar influences on climate. Rev. Geophys. 48, RG4001.
Griffiths, M.L., 2009. Increasing Australian-Indonesian monsoon rainfall linked to early Holocene sea-level rise. Nat. Geosci. 2, 636–639.
Grove, J., 2004. Little Ice Ages: Ancient and Modern. Routledge, New York.
Gupta, A.K., Anderson, D.M., Overpeck, J.T., 2003. Abrupt changes in the Asian southwest monsoon during the Holocene and their links to the North Atlantic Ocean. Nature 421, 354–357.
Gupta, A.K., Das, M., Anderson, D.M., 2005. Solar influence on the Indian summer monsoon during the Holocene. Geophys. Res. Lett. 32. doi:10.1029/2005GL022685.
Hall, B.L., 2009. Holocene glacial history of Antarctica and the sub-Antarctic islands. Quaternary Sci. Rev. 28, 2213–2230.
Hall, I.R., Bianchi, G.G., Evans, J.R., 2004. Centennial to millennial scale Holocene climate-deep water linkage in the North Atlantic. Quaternary Sci. Rev. 23, 1529–1536.
Hannesdóttir, H., 2006. Reconstructing environmental change in South Iceland during the last 12,000 years based on sedimentological and seismostratigraphical studies in Lake Hestvatn. M.S. thesis, University of Iceland, Reykjavik.
Haug, G.H., Hughen, K.A., Sigman, D.M., Peterson, L.C., Röhl, U., 2001. Southward migration of the intertropical Convergence zone through the olocene. Science 293, 1304–1308.

Heikkilä, M., Seppä, H.A., 2003. 11,000 yr palaeotemperature reconstruction from the southern boreal zone in Finland. Quaternary. Sci. Rev. 22, 541–554.
Heusser, C.J., 1960. Late Pleistocene environments of the Laguna de San Rafael area, Chile. Geogr. Rev. 50, 555–577.
Heusser, C.J., 1964. Some pollen profiles from the Laguna de San Rafael area, Chile, Ancient Pacific Floras. University of Hawaii Press, pp. 95–114.
Hodell, D.A., Curtis, J.H., Brenner, M., 1995. Possible role of climate in the collapse of Classic Maya civilization. Nature 375, 391–394.
Holmgren, K., Lee-Thorp, J.A., Cooper, G.J., Lundbland, K., Partridge, T.C., Scott, L., Sithaldeen, R., Talma, A.S., Tyson, P.D., 2003. Persistent millennial-scale climatic variability over the past 25,000 years in Southern Africa. Quaternary. Sci. Rev. 22, 2311–2326.
Holzhauser, H., Zumbühl, H.J., 1999. Glacier fluctuations in the western Swiss and French Alps in the 16th century. Climatic Change 43, 223–237.
Holzhauser, H., 1997. Fluctuations of the Grosser Aletsch glacier and the Gorner glacier during the last 3200 years, new results. In: Frenzel, B., Boulton, G.S., Gläser, B., Huckreide, U. (Eds.), Glacier fluctuations during the Holocene. Gustav Fischer, Stuttgart, pp. 35–58.
Holzhauser, H., 1995. Gletscherschwankungen innerhalb der letzten 3200 Jahre am Beispiel des Grossen Aletsch- und des Gornergletschers. Neue Ergebnisse. In: Gletscher im ständigen Wandel. Publikationen der Schweizerischen Akademie der Naturwissenschaften, vol. 6, pp. 101–123.
Holzhauser, H., Magny, M., Zumbühl, H.J., 2005. Glacier and lake-level variations in west-central Europe over the last 3500 years. The Holocene 15, 789–801.
Hong, Y.T., Hong, B., Lin, Q.H., Shibata, Z., Hirota, M., Uchida, M., Leng, X.T., Jiang, H.B., Xu, H., Wang, H., Yi, L., 2003. Correlation between Indian Ocean summer monsoon and north Atlantic climate during the Holocene. Earth Planet. Sc. Lett. 211, 371–380.
Hong, Y.T., Hong, B., Lin, Q.H., Shibata, Z., Hirota, M., Zhu, Z.X., Leng, X.T., Wang, Y., Wang, H., Yi, L., 2005. Inverse phase oscillations between the East Asian and Indian Ocean summer monsoons during the last 12000 years and paleo-El Niño. Earth Planet. Sci. Lett. 231, 337–346.
Hormes, A., Beer, J., Schlüchter, C., 2006. A geochronological approach to understanding the role of solar activity on Holocene glacier length variability in the Swiss Alps. Geogr. Ann. A 88, 281–294.
Hormes, A., Müller, B.U., Schlüchter, C., 2001. The Alps with little ice: evidence for eight Holocene phases of reduced glacier extent in the Central Swiss Alps. Holocene 11, 255–265.
Hormes, A., Schlüchter, C., Stocker, T.F., 1998. Minimal extension phases of Unteraarglacier (Swiss Alps) during the Holocene based on 14C analysis of wood. Radiocarbon 40, 809–817.
Hu, C., Henderson, G.M., Huang, J., Xie, S., Sun, Y., Johnson, K.R., 2008. Quantification of Holocene Asian monsoon rainfall from spatially separated cave records. Earth Planet. Sc. Lett. 266, 221–232.
Hu, F.S., Kaufmann, D., Yoneji, S., Nelson, D., Shemesh, A., Huang, Y., Tian, J., Bond, G., Clegg, B., Brown, T., 2003. Cyclic variation and solar forcing of Holocene climate in the Alaskan Subarctic. Science 301, 1890–1893.
Huang, S.P., Pollack, H.N., Shen, P.-Y., 2008. A late Quaternary climate reconstruction based on borehole heat flux data, borehole temperature data, and the instrumental record. Geophys. Res. Lett. 35. doi:10.1029/2008GL034187.
Hughes, M.K., Graumlich, L.J., 1996. Climatic variations and forcing mechanisms of the last 2000 years. NATO ASI Ser. 141, 109–124.
Hughes, M.K., Diaz, H.F., 1994. Was there a "Medieval Warm Period", and if so, where and when? Climatic Change 26, 109–142.
Humlum, O., Elberling, B., Hormes, A., Fjordheim, K., Hansen, O.H., Heinemeier, J., 2005. Late-Holocene glacier growth in Svalbard, documented by subglacial relict vegetation and living soil microbes. Holocene 15, 396–407.
Ingòlfsson, O., Frich, P., Funder, S., Humlum, O., 1990. Palaeoclimatic implications of an early Holocene glacier advance on Disko Island, west Greenland. Boreas 19, 297–311.
IPCC (Intergovernmental Panel on Climate Change), 2007. Climate Change 2007: The Physical Science Basis. Cambridge University Press, Cambridge and New York.
IPCC (Intergovernmental Panel on Climate Change), 2001. Climate Change: The Scientific Basis. Cambridge University Press, Cambridge and New York.
Isono, D., Yamamoto, M., Irino, T., Oba, T., Murayama, M., Nakamura, T., Kawahata, H., 2009. The 1500-year climate oscillation in the midlatitude North Pacific during the Holocene. Geology 37, 591–594.
Ivy-Ochs, S., Kerschner, H., Maisch, M., Christl, M., Kubik, P.W., Schlüchter, C., 2009. Latest Pleistocene and Holocene glacier variations in the European Alps. Quaternary Sci. Rev. 28, 2137–2149.
Jennings, A.E., Knudsen, K.L., Hals, M., Hansen, C.V., Andrews, J.T., 2002. A mid-Holocene shift in Arctic sea-ice variability on the East Greenland Shelf. Holocene 12, 49–58.
Joerin, U.E., Nicolussi, K., Fischer, A., Stocker, T.F., Schlüchter, C., 2008. Holocene optimum events inferred from subglacial sediments at Tschierva Glacier, Eastern Swiss Alps. Quaternary Sci. Rev. 27, 337–350.
Joerin, U.E., Stocker, T.F., Schlüchter, C., 2006. Multicentury glacier fluctuations in the Swiss Alps during the Holocene. Holocene 16, 697–704.
Johnsen, S.J., Clausen, H.B., Dansgaard, W., Gundestrup, N.S., Hammer, C.U., Andersen, U., Andersen, K.K., Hvidberg, C.S., Dahl-Jensen, D., Steffensen, J.P., Shoji, H., White, J., Jouzel, J., Fishe, D., 1997. The δ18O record along the Greenland Ice Core Project deep ice core and the problem of possible Eemian climatic instability. J. Geophys. Res. 102, 26,397–26,410.
Jouzel, J., Masson-Delmotte, V., Cattani, O., Dreyfus, G., Falourd, S., Hoffmann, G., Minster, B., Nouet, J., Barnola, J.M., Chappellaz, J., Fischer, H., Gallet, J.C., Johnsen, S., Leuenberger, M., Loulergue, L., Luethi, D., Oerter, H., Parrenin, F., Raisbeck, G., Raynaud, D., Schilt, A., Schwander, J., Selmo, E., Souchez, R., Spahni, R., Stauffer, B., Steffensen, J.P., Stenni, B., Stocker, T.F., Tison, J.L., Werner, M., Wolff, E.W., 2007. Orbital and millennial Antarctic climate variability over the past 800,000 years. Science 317, 793–796.
Karlén, W., Fastook, J.L., Holmgren, K., Malmstroem, M., Matthews, J.A., Odada, E., Risberg, J., Rosquist, G., Sandgren, P., Shemesh, A., Westerberg, L.-O., 1999. Glacier fluctuations on Mount Kenia since ca 6000 cal.years BP: implications for Holocene climatic change in Africa. Ambio 28, 409–418.
Kaufman, D.-S., 29 co-authors, 2004. Holocene thermal maximum in the western Arctic (0-180°W). Quaternary Sci. Rev. 23, 529–560.
Kaufman, D.S., Schneider, D.P., McKay, N.P., Ammann, C.M., Bradley, R.S., Briffa, K.R., Miller, G.H., Otto-Bliesner, B.L., Overpeck, J.T., Vinther, B.M., Arctic Lakes 2k Project Members, (Abbott, M., Axford, Y., Bird, B., Birks, H.J.B., Bjune, A.E., Briner, J., Cook, T., Chipman, M., Francus, P., Gajewski, K., Geirsdóttir, Á, Hu, F.S., Kutchko, B., Lamoureux, S., Loso, M., MacDonald, G., Peros, M., Porinchu, D., Schiff, C., Seppä, H., Thomas, E.), 2009. Recent warming reverses long-term Arctic cooling. Science 325, 1236–1239.
Kelly, M.A., 1988. The status of the Neoglacial in western Greenland. Grunlands Geologiske Undersшgelse Rapport 96.
Kelly, M.A., Lowell, T.V., 2009. Fluctuations of local glaciers in Greenland during latest Pleistocene and Holocene time. Quaternary Sci. Rev. 28, 2088–2106.
Kim, J.-H., Rimbu, N., Lorenz, S.J., Lohmann, G., Nam, S.-I., Schouten, S., Rühlemann, C., Schneider, R.R., 2004. North Pacific and North Atlantic sea-surface temperature variability during the Holocene. Quaternary Sci. Rev. 23, 2141–2154.
King, L., 1974. Studien zur postglazialen Gletscher- und Vegetationsgeschichte des Sustenpassgebietes. Basler Beitr. z. Geographie 18, 1–123.
Kirkbride, M.P., Dugmore, A.J., 2006. Responses of mountain lee caps in central Iceland to Holocene climate change. Quarternary Sci. Rev. 25, 1692–1707.
Klimenko, V.V., Klimanov, V.A., Fedorov, M.V., 1996. The history of the mean temperature of the Northern Hemisphere over the last 11,000 years. Trans. Russ. Acad. Sci. 4, 626–629.
Krivova, N.A., Solanki, S.K., 2008. Models of solar irradiance variations: Current status. Astron. Astrophys. 29, 151–158.
Kuylenstierna, J.L., Rosquist, G.C., Holmlund, P., 1996. Late-Holocene glacier variations in the Cordillera Darwin, Tierra del Fuego. Holocene 6, 353–358.
Lamy, F., Arz, H.W., Bond, G.C., Bahr, A., Pätzold, J., 2006. Multicentennial-scale hydrological changes in the Black Sea and northern Red Sea during the Holocene and the Arctic/North Atlantic oscillation. Paleoceanography 21, PA1008.
Langdon, P.G., Barber, K.E., Hughes, P.D.M., 2003. A 7500-year peat-based palaeoclimatic reconstruction and evidence for an 1100-year cyclicity in bog surface wetness from Temple Hill Moss, Pentland Hill, southeast Scotland. Quaternary Sci. Rev. 22, 259–274.
Larocque, I., Hall, R.I., 2004. Holocene temperature estimates and chironomid community composition in the Abisko Valley, northern Sweden. Quaternary. Sci. Rev. 23, 2453–2465.
Larrasoaña, J.C., Roberts, A.P., Rohling, E.J., Winkelhofer, M., Wehausen, R., 2003. Three million years of monsoon variability over the northern Sahara. Clim. Dynam. 21, 689–698.
Lauritzen, S.-E., Lundberg, J., 1999. Calibration of the speleothem delta function: an absolute temperature record for the Holocene in northern Norway. Holocene 9, 659–669.
LeGrande, A.N., Schmidt, G.A., 2008. Ensemble, water isotope-enabled, coupled general circulation modeling insights into the 8.2 ka event. Paleoceanography 23. doi:10.1020/2008PA001610.
Lehmkuhl, F., 1997. Late Pleistocene, Late-glacial and Holocene glacier advances on the Tibetan Plateau. Quatern. Int. 38/39, 77–83.
Li, Y.-X., Yu, Z., Kodama, K., 2007. Sensitive moisture response to Holocene millennial-scale climate variations in the Mid-Atlantic region, USA. Holocene 17, 3–8.
Licciardi, J.M., Schaefer, J.M., Taggart, J.R., Lund, D.C., 2006. Holocene glacier fluctuations in the Peruvian Andes indicate northern climate linkages. Science 325, 1677. doi:10.1126/science.1175010.
Ljungqvist, F.C., 2010. A new reconstruction of temperature variability in the extra-tropical Northern Hemisphere during the last two millennia. Geogr. Ann. 92A, 339–351.
Lubinsky, D.J., Forman, S.L., Miller, G.H., 1999. Holocene glacier and climate fluctuations on Franz Josef Land, Arctic Russia, 80°N. Quaternary Sci. Rev. 18, 87–108.
Mangini, A., Verdes, P., Spötl, C., Scholz, D., Vollweiler, N., Kromer, B., 2007. Persistent influence of the North Atlantic hydrography on central European winter temperature during the last 9000 years. Geophys. Res. Lett. 34, L02704. doi:10.1029/2006GL028600.
Mann, M.E., Zhang, Z., Rutherford, S., Bradley, R.S., Hughes, M.K., Shindell, D., Ammann, C., Faluvegi, G., Ni, F., 2009. Global signatures and dynamical origins of the little ice age and medieval climate anomaly. Science 326, 1256–1260.
Mark, B., Seltzer, G., Rodbell, D., Goodman, A., 2002. Rates of deglaciation during the Last Glaciation and Holocene in the Cordillera Vilcanota-Quelccaya ice Cap region, southeastern. Peru. Quaternary Res. 57, 287–298.
Masiokas, M.H., Luckman, B.H., Villalba, R., Delgado, S., Skvarca, P., Ripalta, A., 2008. Little Ice Age fluctuations of small glaciers in the Monte Fitz Roy and Lago del Desierto areas, south Patagonian Andes, Argentina. Palaeogeogr. Palaeocl.. doi:10.1016/j.palaeo.2007.10.031.
Masson, V., Vimeux, F., Jouzel, J., Morgan, V., Delmotte, M., Ciais, P., Hammer, C., Johnsen, S., Lipenkov, V.Y., Mosley-Thompson, E., Petit, J.-R., Steig, E.J.,

Stievenard, M., Vaikmar, R., 2000. Holocene climate variability in Antarctica based on 11 ice-core isotopic records. Quaternary Res. 54, 348–358.
Matthews, J.A., Briffa, K.R., 2005. The 'Little ice age': Re-evaluation of an evolving concept. Geogr. Ann. A, 17–36.
Matthews, J.A., Dresser, P.Q., 2008. Holocene glacier variation chronology of the Smorstabbtinden massif, Jotunheimen, southern Norway, and the recognition of century- to millennial-scale European Neoglacial events. Holocene 18, 181–201.
Mayewski, P.A., Rohling, E.E., Stager, J.C., Karlen, W., Maasch, K.A., Meeker, L.D., Meyerson, E.A., Gasse, F., van Kreveld, S., Holmgren, K., Lee-Thorp, J., Rosqvist, G., Rack, F., Staubwasser, M., Schneider, R.R., Steig, E.J., 2004. Holocene climate variability. Quaternary Res. 62, 243–255.
Menounos, B., Osborn, G., Clague, J.J., Luckman, B.H., 2009. Latest Pleistocene and Holocene glacier fluctuations in western Canada. Quaternary Sci. Rev. 28, 2049–2074.
Mercer, J.H., 1982. Holocene glacier variations in southern Patagonia. Striae 18, 35–40.
Mercer, J.T., 1968. Variations of some Patagonian glaciers since the Late-Glacial. Am. J. Sci. 266, 91–109.
Miller, G.H., 1973a. Variations in lichen growth from direct measurements: preliminary curves for Alectoria minuscula from eastern Baffin Island, N.W.T. Canada. Arctic Alpine Res. 5, 333–339.
Miller, G.H., 1973b. Late-Quaternary glacial and climatic history of northern Cumberland peninsula, Baffin Island, N.W.T. Canada. Quaternary Res. 3, 561–583.
Miller, G.H., Wolfe, A.P., Briner, J.P., Sauer, P.E., Nesje, A., 2005. Holocene glaciation and climate evolution of Baffin Island, Arctic Canada. Quaternary Sci. Rev. 24, 1703–1721.
Moros, M., Andrews, J.T., Eberl, D.D., Jansen, E., 2006. Holocene history of drift ice in the Northern North Atlantic: evidence for different spatial and temporal modes. Paleoceanography 21. doi:10.1029/2005PA001214.
Nesje, A., 2009. Latest Pleistocene and Holocene alpine glacier fluctuations in Scandinavia. Quaternary Sci. Rev. 28, 2119–2136.
Nesje, A., Matthews, J.A., Dahl, S.O., Berrisford, M.S., Andersson, C., 2001. Holocene glacier fluctuations of Flatebreen and winter-precipitation changes in the Jostedalsbree region, western Norway, based on glaciolacustrine sediment records. Holocene 11, 267–280.
Nicolussi, K., Patzelt, G., 2001. Untersuchungen zur holozänen Gletscherentwicklung von Pasterze und Gepatschferner (Ostalpen). Z. Gletscherkd. Glazialgeol. 36, 1–87.
Niggemann, S., Mangini, A., Mudelsee, M., Richter, D.K., Wurth, G., 2003. Sub-Milankovitch climatic cycles in Holocene stalagmites from Sauerland, Germans. Earth Planet. Sci. Lett. 216, 539–547.
O'Brien, S.R., Mayewski, P.A., Meeker, L.D., Meese, D.A., Twickler, M.S., Whitlow, S.I., 1995. Complexity of Holocene climate as reconstructed from a Greenland ice core. Science 270, 1962–1964.
Oerlemans, J., 2005. Extracting a climate signal from 169 glacier records. Science 308, 675–677.
Oppo, D.W., McManus, J.F., Cullen, J.L., 2003. Deepwater variability in the Holocene epoch. Nature 422, 277–278.
Osborn, G., Menounos, B., Koch, J., Clague, J.J., Vallis, V., 2007. Multi-proxy record of Holocene glacial history of the Spearhead and Fitzsimmons ranges, southern Coast mountains, British Columbia. Quaternary. Sci. Rev. 26, 479–493.
Parker, A.G., Goudie, A.S., Stokes, S., White, K., Hodson, M.J., Manning, M., Kennet, D., 2006. A record of Holocene climate change from lake geochemical analyses in southeastern Arabia. Quaternary Res. 66, 465–476.
Patzelt, G., Bortenschlager, S., 1973. Die postglazialen Gletscher- und Klimaschwankungen in der Venedigergruppe (Hohe Tauern, Ostalpen). Z. Geomorphol.N.F. (16), 25–72. Suppl.bd.
Patzelt, G., 1977. Der zeitliche Ablauf und das Ausmass postglazialer Klimaschwankungen in den Alpen. In: Frenzel, B. (Ed.), Dendrochronologie und postglaziale Klimaschwankungen in Europa, Erdwiss. Forschung, vol. 13, pp. 249–259.
Pelejero, C., Grimalt, J.O., Heilig, S., Kienast, M., Wang, L., 1999. High-resolution UK37 temperature reconstructions in the South China Sea over the past 220 kyr. Paleoceanography 14, 224–231.
Petit, J.R., Jouzel, J., Raynaud, D., Barkov, N.I., Barnola, J.-M., Basile, I., Bender, M., Chappellaz, J., Davis, M., Delaygue, G., Delmotte, M., Kotlyakov, V.M., Legrand, M., Lipenkov, V.Y., Lorius, C., Pepin, L., Ritz, C., Saltzman, E., Stievenard, M., 1999. Climate and atmospheric history of the past 420,000 years from the Vostok ice core, Antarctica. Nature 399, 429–436.
Pfister, C., 1995. Monthly temperature and precipitation in central Europe from 1529–1979: quantifyingdocumentary evidence on weather and its effects. In: Bradley, R.S., Jones, P.D. (Eds.), Climate since AD 1500. Routledge, London and New York, pp. 118–142.
Plunkett, G.M., Pilcher, J.R., McCormac, F.G., Hall, V.A., 2004. New dates for first millennium BC tephra isochrones in Ireland. The Holocene 14, 780–786.
Polyak, L., Murdmaa, I., Ivanova, E., 2004. A high-resolution, 800-year glaciomarine record from Russkaya Gavan, a Novaya Zemlya fjord, eastern Barents Sea. Holocene 14, 628–634.
Porter, S.C., Denton, G.H., 1967. Chronology of neoglaciation in the north American Cordillera. Am. J. Sci. 265, 177–210.
Principato, S., 2008. Geomorphic evidence for Holocene glacial advances and sea level fluctuations on eastern Vestfirðir, northwest Iceland. Boreas 37, 132–145.
Pu, Q., 1991. Evolution of natural environment in China since the last glacial period and its position in the global changes. Quaternary Sci. 3, 245–259.
Renner, F., 1982. Beiträge zur Gletschergeschichte des Gotthardgebietes und dendroklimatologische Analysen an fossilen Hölzern. Phys. Geographie 8, 1–180.
Renssen, H., Goosse, H., Fichefet, T., 2007. Simulation of Holocene cooling events in a coupled climate model. Quaternary Sci. Rev. 26, 2019–2029.
Renssen, H., Seppä, H., Heiri, O., Roche, D.M., Goosse, H., Fichefet, T., 2009. The spatial and temporal complexitiy of the Holocene thermal maximum. Nat. Geosci. 2, 411–414.
Risebrobakken, B., Jansen, E., Andersson, C., Mjelde, E., Hevrøy, K., 2003. A high-resolution study of Holocene paleoclimatic and paleoceanographic changes in the Nordic Seas. Paleoceanography 18, 1017–1031.
Rodbell, D.T., 1992. Lichenometric and radiocarbon dating of Holocene glaciation, Cordillera Blanca, Peru. Holocene 2, 19–29.
Rohling, E.J., Pälike, H., 2005. Centennial-scale climate cooling with a sudden cold event around 8200 years ago. Nature 434, 975–979.
Rosqvist, G., Schuber, P., 2003. Millennial-scale climate changes on south Georgia, southern ocean. Quaternary Res. 59, 470–475.
Rosqvist, G., Jonsson, C., Yam, R., Karlén, W., Shemesh, A., 2004. Diatom oxygen isotopes in pro-glacial lake sediments from northern Sweden: a 5000 year record of atmospheric circulation. Quaternary Sci. Rev. 23, 851–859.
Röthlisberger, F., 1987. 10,000 Jahre Gletschergeschichte der Erde. Verlag Sauerländer, Aarau, 348 pp.
Röthlisberger, F., Geyh, M., 1985. Glacier variations in Himalayas and Karakoram. Z. Gletscherkd. Glazialgeol 21, 237–249.
Röthlisberger, F., Haas, P., Holzhauser, H., Keller, W., Bircher, W., Renner, F., 1980. Holocene climatic fluctuations-Radiocarbon dating of fossil soils (fAh) and woods from moraines and glaciers in the Alps. Geogr. Helv. 35, 21–52.
Röthlisberger, H., Oeschger, H., 1961. Datierung eines ehemaligen Standes des Aletschgletschers durch Radioaktivitätsmessung an Holzproben und Bemerkungen zu Holzfunden an weiteren Gletschern. Z. Gletscherkd. Glazialgeol. 4, 191–205.
Russell, J.M., Johnson, T.C., 2005. Late Holocene climate change in the North Atlantic and equatorial Africa: millennial-scale ITCZ migration. Geophys. Res. Lett. 32, L17705.
Schaefer, J.M., Denton, G.H., Kaplan, M., Putnam, A., Finkel, R.C., Barrell, D.J.A., Andersen, B.G., Schwartz, R., Mackintosh, A., Chinn, T., Schlüchter, C., 2009. High-Frequency Holocene glacier fluctuations in New Zealand differ from the northern signature. Science 324, 622. doi:10.1126/science.1169312.
Schefuss, E., Schouten, S., Schneider, R.R., 2005. Climatic controls on central African hydrology during the past 20,000 years. Nature 437, 1003–1006.
Schettler, G., Liu, Q., Mingram, J., Stebich, M., Dulski, P., 2006. East-Asian monsoon variability between 15000 and 2000 cal. yr BP recorded in varved sediments of Lake Sihailongwan (northeastern China, Long Gang volcanic field). Holocene 16, 1043–1057.
Schneebeli, W., Röthlisberger, F., 2000. 8000 Jahre Walliser Gletschergeschichte. Die Alpen 52, 1–152.
Seltzer, G., Rodbell, D., Burns, S., 2000. Isotopic evidence for late Quaternary climatic change in tropical South America. Geology 28, 35–38.
Seong, Y.B., Owen, L.A., Yi, C., Finkel, R.C., 2009. Quaternary glaciation of Muztag Ata and Kongur Shan: evidence for glacier response to rapid climate changes throughout the Late-glacial and Holocene in westernmost Tibet. Geol. Soc. Am. Bull. 129. doi:10.1130/B26339.1.
Seppä, H., Birks, H.J.B., 2002. Holocene Climate reconstructions from the Fennoscandian tree-line area based on pollen data from Toskaljavri. Quaternary Res. 57, 191–199.
Seppä, H., Birks, H.J.B., 2001. July mean temperature and annual precipitation trends during the Holocene in the Fennoscandian tree-line area: pollen-based climate reconstructions. Holocene 11, 527–539.
Seppä, H., Birks, H.J.B., Giesecke, T., Hammarlund, D., Alenius, T., Antonsson, K., Bjune, A.E., Heikkilä, M., MacDonald, G.M., Ojala, A.E.K., Telford, R.J., Veski, S., 2007. Spatial structure of the 8200 cal yr BP event in northern Europe. Clim. Past 3, 225–236.
Seppä, H., Hammarlund, D., Antonsson, K., 2005. Low-frequency and high-frequency changes in temperature and effective humidity during the Holocene in south-central Sweden: implications for atmospheric and oceanic forcings of climate. Clim. Dynam. 25, 285–297.
Seppä, H., Poska, A., 2004. Holocene annual mean temperature changes in Estonia and their relationship to solar insolation and atmospheric circulation patterns. Quaternary Res. 61, 22–31.
Shevenell, A.E., Ingalls, A.E., Domack, E.W., 2007. Orbital and atmospheric forcing of western Antarctic Peninsula climate in the Holocene: The TEX86 paleotemperature record of Palmer Deep. U.S. Geological Survey and The National Academies.
Solomina, O., Jomelli, V., Kaser, G., Ames, A., Berger, B., Pouyaud, B., 2007. Lichenometry in the Cordillera Blanca, Peru: "Little ice age" moraine chronology. Glob. Planet. Change 59, 225–235.
Speranza, A., van Geel, B., van der Pflicht, J., 2002. Evidence for solar forcing of climate change at ca. 850 cal BC from a Czech peat sequence. Glob. Planet. Change 35, 51–65.
Stager, J.C., Mayewski, P.A., Meeker, L.D., 2002. Cooling cycles, Heinrich event 1, and the desiccation of Lake Victoria. Palaegeogr. Palaeocl. 183, 169–178.
Staubwasser, M., Sirocko, F., Grootes, P.M., Segl, M., 2003. Climate change at the 4.2ka BP termination of the Indus valley civilization and Holocene south Asian monsoon variability. Geophys. Res. Lett. 30, 1425–1432.
Steig, E.J., Morse, D.L., Waddington, E.D., Stuiver, M., Grootes, P.M., Mayewski, P.A., Twickler, M.S., Whitlow, S.I., 2000. Wisconsinan and Holocene climate history

from an ice core at Taylor Dome, western Ross Embayment, Antarctica. Geogr. Ann. 82, 213–225.
Steig, E.J., Brook, E.J., White, J.W.C., Sucher, C.M., Bender, M.L., Lehmann, S.J., Morse, D.L., Waddington, E.D., Clow, G.D., 1998. Synchronous climate changes in Antarctica and the north Atlantic. Science 282, 92–95.
Steinhilber, F., Beer, J., Fröhlich, C., 2009. Total solar irradiance during the Holocene. Geophys. Res. Lett. 36. doi:10.1029/2009GL040142.
Stott, L., Timmermann, A., Thunell, R., 2007. Southern Hemisphere and deep-sea warming led deglacial atmospheric CO2 rise and topical warming. Science 318, 436–438.
Stotter, J., Wastl, M., Caseldine, C., Haberle, T., 1999. Holocene palaeoclimatic reconstructions in Northern Iceland: approaches and results. Quaternary Sci. Rev. 18, 457–474.
Strelin, J.A., Malagnino, E.C., 2000. Late-glacial history of Lago Argentino, Argentina, and age of the Puerto Bandera moraines. Quaternary Res. 54, 339–347.
Strelin, J., Sone, T., Mori, J., Torielli, C., Nakamura, T., 2006. New data related to Holocene landform development and climatic change from James Ross Island, Antarctic Peninsula. In: Futterer, D.K., Damaske, D., Kleinschmidt, G., Miller, H., Tessensohn, F. (Eds.), Contributions to Global Earth Sciences. Springer-Verlag, New York, pp. 455–460. Antarctica.
Suter, J., 1981. Gletschergeschichte des Oberengadins: Untersuchung von Gletscherschwankungen in der Err- Julier-Gruppe. Phys. Geographie 2, 1–170.
Svendsen, J.I., Mangerud, J., 1997. Holocene glacial and climatic variations on Spitsbergen, Svalbard. Holocene 7, 45–57.
Swindles, G.T., Plunkett, G., Roe, H.M., 2007. A delayed climatic response to solar forcing at 2800 cal. BP: multiproxy evidence from three Irish peatlands. Holocene 17, 177–182.
Tarasov, P.E., Bezukova, E.V., Krivonogov, S.K., 2009. Late Glacial and Holocene changes in vegetation cover and climate in southern Siberia derived from a 15 kyr long pollen record from Lake Kotokel. Clim. Past 5, 285–295.
Thompson, D.P., Menounos, B., Osborn, G., 2009. Holocene and latest Pleistocene alpine glacier fluctuations: a global perspective. Quaternary Sci. Rev. 28, 2021–2033.
Thompson, L.G., Mosley-Thompson, E., Davis, M.E., Henderson, K.A., Brecher, H.H., Zagorodnov, V.S., Mashiotta, T.A., Lin, P.-N., Mikhalenko, V.N., Hardy, D.R., Beer, J., 2002. Ice core records: evidence of Holocene climate change in tropical Africa. Science 298, 589–593.
Thompson, L.G., Mosley-Thompson, E., Davis, M.E., Lin, P.-N., Henderson, K.A., Cole-Dai, J., Bolzan, J.F., Liu, K.-B., 1995. Late glacial stage and Holocene tropical ice core records from Huascaran, Peru. Science 269, 46–50.
Trouet, V., Esper, J., Graham, N.E., Baker, A., Scourse, J.D., Frank, D.C., 2009. Persistent positive north Atlantic oscillation mode dominated the medieval climate anomaly. Science 324, 78–80.
Turney, C., Baillie, M., Clemens, S., Brown, D., Palmer, J., Pilcher, J., Reimer, P., Leuschner, H.H., 2005. Testing solar forcing of pervasive Holocene climate cycles. J. Quaternary Sci. 20, 511–518.
van Geel, B., Bokovenko, N.A., Burova, N.D., Chugunov, K.V., Dergachev, V.A., Dirksen, V.G., Kulkova, M., Nagler, A., Parzinger, H., van der Pflicht, J., Vasiliev, S.S., Zaitseva, G.I., 2004. Climate change and the expansion of the Scythian culture after 850 BC, a hypothesis. J. Archeol. Sci. 31, 1735–1742.
van Geel, B., Heusser, C.J., Renssen, H., Schuurmans, C.J.E., 2000. Climatic change in Chile at around 2700 BP and global evidence for solar forcing: a hypothesis. Holocene 10, 659–664.
Viau, A.E., Gajewski, K., Sawada, M.C., Fines, P., 2006. Millennial-scale temperature variations in North America during the Holocene. J. Geophys. Res. 111. doi:10.1029/2005JD006031.
Viau, A.E., Gajewski, K., Fines, P., Atkinson, D.E., Sawada, M.C., 2002. Widespread evidence of 1500 yr climate variability in North America during the past 14,000 yr. Geology 30, 455–458.
Vinther, B.M., Clausen, H.B., Johnson, S.J., Rasmussen, S.O., Andersen, K.K., Buchardt, S.L., Dahl-Jensen, D., Seierstad, I.K., Siggaard-Andersen, M.-L., Steffensen, J.P., Svensson, A., 2006. A synchronized dating of three Greenland ice cores throughout the Holocene. J. Geophys. Res. 111, D13102.
von Grafenstein, U., Erlenkeuser, H., Brauer, A., Jouzel, J., Johnsen, S.J., 1999. A mid-European decadal isotope-climate record from 15,500 to 5000 Years B.P. Science 284, 1654–1657.
Wang, X., Auler, A.S., Edwards, R.L., Cheng, H., Ito, E., Solheid, M., 2006. Interhemispheric anti-phasing of rainfall during the last glacial period. Quaternary Sci. Rev. 25, 3391–3403.
Wang, Y., Cheng, H., Edwards, R.L., He, Y., Kong, X., An, Z., Wu, J., Kelly, M.J., Dykoski, C.A., Li, X., 2005. The Holocene Asian monsoon: links to solar changes and north Atlantic climate. Science 308, 854–857.
Wanner, H., Bütikofer, J., 2008. Holocene Bond Cycles – real or imaginary? Geografie 4/113, 338–349.
Wanner, H., Beer, J., Bütikofer, J., Crowley, T.J., Cubasch, U., Flückiger, J., Goosse, H., Grosjean, M., Joos, F., Kaplan, J.O., Küttel, M., Müller, S., Prentice, I.C., Solomina, O., Stocker, T.F., Tarasov, P., Wagner, M., Widmann, M., 2008. Mid- to late Holocene climate change: an overview. Quaternary Sci. Rev. 27, 1791–1828.
Wanner, H., Ritz, S.P., 2011. A web-based Holocene Climate Atlas (HOCLAT). The atlas is available under. http://www.oeschger.unibe.ch/research/projects/holocene_atlas/.
Weidick, A., 1996. Late Holocene and historical changes of glacier cover and related relative sea level in Greenland. Z. Gletscherkd. Glazialgeol. 32, 217–224.
Weidick, A., 1968. Observations on some Holocene glacier fluctuations in west Greenland. Meddelelser Om Groenland 165, 1–202.
Weidick, A., Kelly, M., Bennike, O., 2004. Late Quaternary development of the southern sector of the Greenland Ice Sheet, with particular reference to the Qassimiut lobe. Boreas 33, 284–299.
Weijers, J.W.H., Schefuss, E., Schouten, S., Sinninghe Damste, J.S., 2007. Coupled thermal and hydrological evolution of tropical Africa over the Last Deglaciation. Science 315, 1701–1704.
Weiss, H., Courtney, M.-A., Wetterstrom, W., Guichard, F., Senior, L., Meadow, R., Curnow, A., 1993. The genesis and collapse of third millennium north Mesopotamian civilization. Science 261, 995–1004.
Weldeab, S., Lea, D.W., Schneider, R.R., Andersen, N., 2007. 155,000 Years of West African Monsoon and ocean thermal evolution. Science 316, 1303–1307.
Werner, A., 1993. Holocene moraine chronology, Spitsbergen, Svalbard: lichenometric evidence for multiple Neoglacial advantages in the Arctic. Holocene 3, 128–137.
Willard, D.A., Bernhardt, C.E., Korejwo, D.A., Meyers, S.R., 2005. Impact of millennial-scale Holocene climate variability on eastern North American terrestrial ecosystems: pollen-based climatic reconstruction. Glob. Planet. Change 47, 17–35.
Williams, P.W., King, D.N.T., Zhao, J.-X., Collerson, K.D., 2005. Late Pleistocene to Holocene composite speleothem 18O and 13C chronologies from south Island, New Zealand – did a global Younger Dryas really exist? Earth Planet. Sci. Lett. 230, 301–317.
Winkler, S., Matthews, J.A., 2010. Holocene glacier chronologies: are high-resolution global and interhemispheric comparisons possible? Holocene 20, 1137–1147.
Xiao, J., Chang, Z., Wen, R., Zhai, D., Itoh, S., Lomtatidze, Z., 2009. Holocene weak monsoon intervals indicated by low lake levels at Hulun Lake in the monsoonal margin region of northeastern Inner Mongolia, China. Holocene 19, 899–908.
Yancheva, G., Nowaczyk, N.R., Mingram, J., Dulski, P., Schettler, G., Negendank, J.F.W., Liu, J., Sigman, D.M., Peterson, L.C., Haug, G.H., 2007. Influence of the intertropical convergenze zone on the East Asian monsoon. Nature 445, 74–77.
Yang, B., Bräuning, A., Dong, Z., Zhang, Z., Keqing, J., 2008. Late Holocene monsoonal temperate glacier fluctuations on the Tibetan Plateau. Glob. Planet. Change 60, 126–140.
Yi, C., Chen, H., Yang, J., Liu, B., Fu, P., Liu, K., Li, S., 2008. Review of Holocene glacial chronologies based on radiocarbon dating in Tibet and its surrounding mountains. J. Quaternary Sci. 23, 533–558.
Yu, Y., Yang, T., Li, J., Liu, J., An, C., Liu, X., Fan, Z., Lu, Z., Li, Y., Su, X., 2006. Millennial-scale Holocene climate variability in the NW China drylands and links to the tropical Pacific and the North Atlantic. Palaeogeogr. Palaeocl. 233, 149–162.
Yu, Z., Campbell, I.D., Campbell, C., Vitt, D.H., Bond, G.C., Apps, M.J., 2003. Carbon sequestration in western Canadian wet-dry climate cycles at millennial scales. Holocene 13, 801–808.
Zhang, J., Chen, F., Holmes, J.A., Li, H., Guo, X., Wang, J., Li, S., Lü, Y., Zhao, Y., Qiang, M., 2011. Holocene monsoon climate documented by ocygen and carbon isotopes from lake sediments and peat bogs in China: a review and synthesis. Quaternary Sci. Rev. 30, 1973–1987.
Zhao, M., Beveridge, N.A.S., Shackleton, N.J., Sarnthein, M., Eglinton, G., 1995. Molecular stratigraphy of cores off northwest Africa: sea surface temperature history over the last 80 ka. Paleoceanography 10, 661–675.
Zhou, S.Z., Chen, F.H., Pan, B.T., Cao, J.X., Li, J.J., Derbyshire, E., 1991. Environmental change during the Holocene in western China on a millennial timescale. Holocene 1, 151–156.
Zielinski, G.A., 2000. Use of paleo-records in determining variability within the volcanism-climate system. Quaternary Sci. Rev. 19, 417–438.
Zoller, H., 1977. Alter und Ausmass postglazialer Klimaschwankungen in den Schweizer Alpen. In: Frenzel, B. (Ed.), Dendrochronologie und postglaziale Klimaschwankungen in Europa, Erdwissenschaftl. Forschung, vol. 13, pp. 271–281.
Zoller, H., Schindler, C., Röthlisberger, H., 1966. Postglaziale Gletscherstände und Klimaschwankungen im Gotthardmassiv und Vorderrheingebiet. In: Verhandl. Naturf. Ges. Basel, vol. 77 97–164.
Zumbühl, H.J., Holzhauser, H., 1988. Alpengletscher in der Kleinen Eiszeit. Die Alpen 64, 129–322.
Zumbühl, H.J., 1980. Die Schwankungen der Grindelwaldgletscher in den historischen Bild- und Schriftquellen des 12. bis 19. Jahrhunderts: Ein Beitrag zur Gletschergeschichte und Erforschung des Alpenraumes, Denkschriften d. Sz. Naturf. Ges. 92, Birkhäuser, Basel. 279 pp.